AD NUMBER

AD848324

LIMITATION CHANGES

TO:

Approved for public release; distribution is unlimited.

FROM:

Distribution authorized to U.S. Gov't. agencies and their contractors; Critical Technology; DEC 1968. Other requests shall be referred to Naval Weapons Center, China Lake, CA 93555. This document contains export-controlled technical data.

AUTHORITY

usnwc ltr, 30 aug 1974

NWC TP 4681

INVESTIGATION OF CONTRAST DEGENERACY WITH INCREASING SCATTER CONCENTRATION FOR A WATER MEDIUM WHEN ILLUMINATED WITH AND WITHOUT A CIRCULARLY POLARIZED SOURCE

by

Gary D. Gilbert

Systems Development Department

ABSTRACT. Luminous flux returns were measured from a black and white painted 5-inch x ½-inch aluminum target placed in a water filled 60 x 30 x 25 cm aquarium illuminated by an external circularly polarized (CP) tungsten projector lamp. Simultaneously, apparent background flux containing backscatter from the illuminating beam was measured with and without a circular analyzer on the Model 2000 Gamma-Scientific telephotometer. Turbidity of the water was controlled by adding varied sizes of polystyrene latex spheres of relative refractive index m = 1.20. Contrasts were determined as a function of particle diameter and amount concentration for six discrete-size spheres ranging from 0.126 microns to 1.099 microns and three size distributions from 6 to 100 microns.

A ratio comparison of the contrasts showed a definite improvement for the smaller diameter spheres, d ≤ 0.557 microns with circularly polarized light. There was only a slight contrast improvement for the 0.796 micron spheres and no improvement for the 1.099 micron spheres. Contrast degraded for CP illuminated scattering from spheres in the 6 to 100 micron diameter range. Considering the ocean's natural scatterers distribution, circular polarization will probably most improve contrast in the vertical region from the lower euphotic zone to a few meters above bottom.

This report is a facsimile of a thesis prepared in partial satisfaction of the requirements for a master's degree of science in engineering. It is published at the working level for information only.

NAVAL WEAPONS CENTER
CHINA LAKE, CALIFORNIA * DECEMBER 1968

NAVAL WEAPONS CENTER
AN ACTIVITY OF THE NAVAL MATERIAL COMMAND

M. R. Etheridge, Capt., USN ..... Commander
Thomas S. Amlie, Ph.D. ..... Technical Director

FOREWORD

This study was one of a series of investigations made toward extending the effective visibility range of underwater photography and television systems. NWC personnel performed the study using Naval Weapons Center equipment; the author then used the information gleaned from the investigation as the material for a thesis in partial satisfaction of the requirements for the degree of Master of Science in Engineering.

The work, performed as part of an official project supported by underwater research project funds, was done during the latter part of CY 1967. The thesis was put into final form at the author's expense. This document is a facsimile of the thesis and is published at the working level for others interested in underwater measurement techniques.

Released by
F. M. ASHBROOK, Head
Instrument Development Division
18 November 1968

Under authority of
IVAR E. HIGHBERG, Head
Systems Development Department

NWC Technical Publication 4681

Published by . . . . . Systems Development Department
Manuscript 30/MS 9-56
Collation . . . . . Cover, 38 leaves, DD Form 1473, abstract cards
First printing . . . . . 180 unnumbered copies
Security classification . . . . . UNCLASSIFIED

CONTENTS

INTRODUCTION
Chapter One

In conjunction with the procurement of the optical sensor suite for the U. S. Navy's Deep Submergence Rescue Vehicle, funds were allocated to the Naval Weapons Center (NAVWPNSCEN), China Lake, California to conduct a study of state-of-the-art methods to extend the effective visibility range of underwater photography and television systems.

The operational depth at which the vehicle is to operate is far below the photic layer where natural illumination penetrates. This implied that all systems investigated needed some type of artificial light source together with the photo-sensitive receiver.

1. Summary of the Underwater Visibility Problem

It soon became apparent that there are two limitations to visibility range for underwater viewing systems. For very clear mote-free waters, as might be found at middle ocean depths, the range at which an object may be seen and/or photographed is dependent only on the illumination level that the light source can provide at the object. This is called the absorption or power limited case. Here the signal information power returned to the receiver is less than the receiver's detectable power threshold. An increase in source power would produce an increase in viewing range.

The second case occurs in more turbid water - rivers, lakes, coastal waters, surface waters in areas of upwelling nutrients, bottom waters with disturbed sediment. In these situations scatterers and motes in the water between the optical source-receiver combination and the object to be viewed backscatter light flux from the source into the receiver. This causes a photon haze or fog to appear. The apparent contrast of the object to its background is reduced and the object disappears into the haze. This apparent contrast C_r is quantitatively expressed as

$$C_r = ({}_tN_r - {}_bN_r)/{}_bN_r$$

where (as shown in Fig. 1) ${}_tN_r$ apparent target radiance at distance r from target t and ${}_bN_r$ apparent radiance of background b at distance r from target t (4,5). The apparent background radiance is given by

$${}_bN_r = T_r\ {}_bN_o + N_r^*\ ,$$

where T_r = transmittance of image forming rays through path length r, ${}_bN_o$ = inherent background radiance in object plane (see Fig.1), and N_r^* = path radiance caused by ambient light and scattered source light seen in length r of the receiver field of view (see Fig. 2). Hence, apparent contrast can be written as

$$C_r = ({}_tN_r - {}_bN_r)/(T_r\ {}_bN_o + N_r^*).$$

For most cases, when r is greater than one attenuation length, $N_r^* \gg T_r\ {}_bN_o$. Any reduction in N_r^* causes a significant increase in C_r. The scattering process limits

contrast by scattering light from the source field into the receiver field of view, causing the path radiance N_r^* to become large. This causes the apparent target contrast to approach zero as the distance r becomes greater. This is called the backscatter or contrast limited case. Here the return power from the object is well above the receiver's power threshold but is not separable from the veiling background luminance. An increase in power produces no increase in range, and may even result in a decrease if the receiver is pushed into a saturation condition.

To alleviate this backscatter limited case various methods and systems were investigated to gate, filter, or otherwise decrease the amount of veiling luminance that reached the receiver. These included the use of circular polarizing filters on the source and receiver, a technique borrowed from atmospheric radar technology.

2. Previous Work With Circular Polarizers

The use of circular polarizing filters for reducing backscatter and improving contrast underwater was verified experimentally in a 24 x 6 x 6 m floating plastic tank at the USNOTS Morris Dam Torpedo Test Range in April 1966 (7).

In the tests, underwater targets were illuminated, photographed, and photometered, both with and without the use of the circular polarization technique. The measured

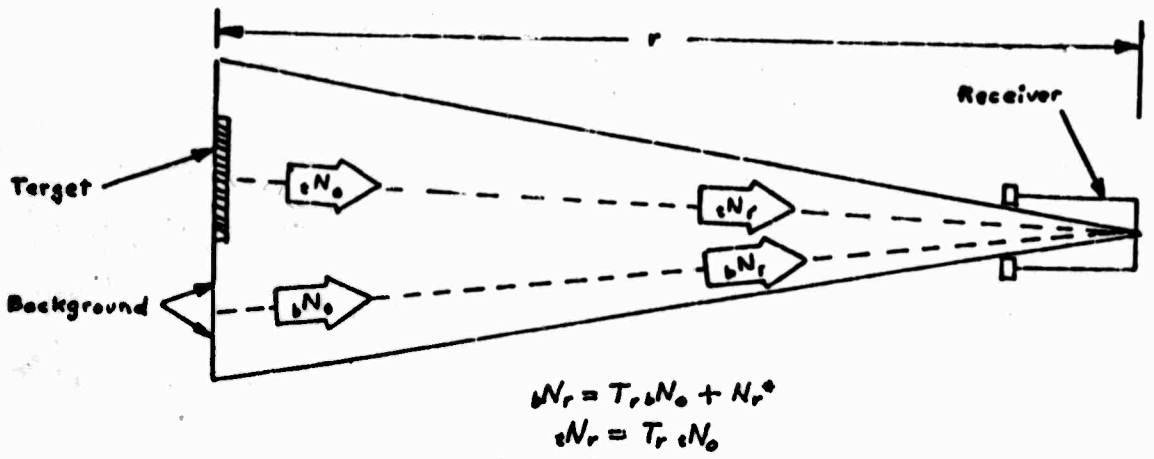

Fig. 1. Geometric representation of target and background radiance traversing distance r to receiver.

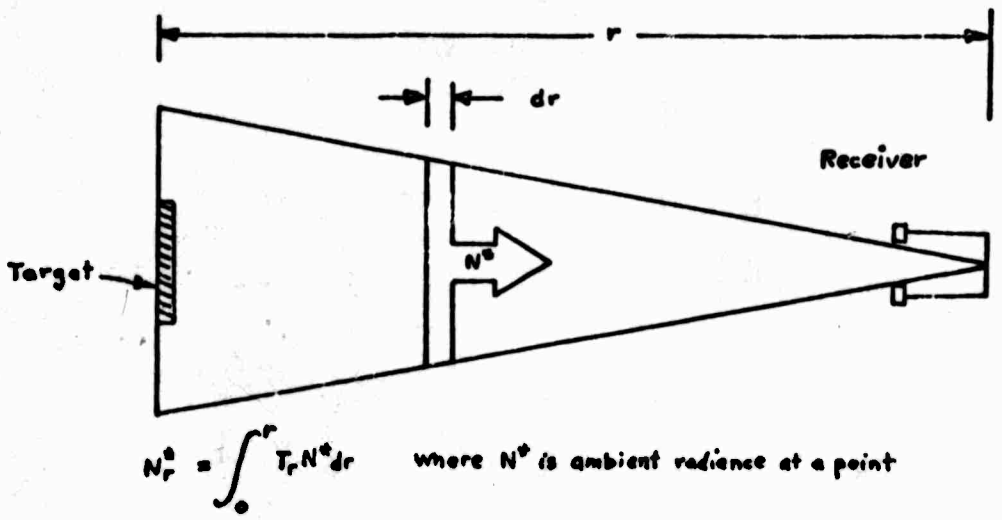

Fig. 2. Representation of path radiance in field of view of receiver caused by ambient light field and scattered flux.

luminances obtained were tabulated, and the average contrast improvement resulting from the use of the circular polarization technique was calculated for a white target against its background and a black target against its background. The contrast improvement ratios varied from 19.5 for the white target to 5.26 for the black target. Circular polarization doubled the range at which the test object could be photographed in the tank. The general trend was a significant improvement in apparent contrast with the use of the circular polarization technique. Experimental laboratory work using artificial scatterers of 0.13μ diameter from the Naugatuck Chemical Corporation, also performed in 1966, showed the same backscatter reduction.

However, swimmer visual observations were also made at coastal beach and surf locations. A hand-held circularly polarized underwater lamp and glass face mask were used by the swimmer. No large apparent increase in object contrasts or visibility ranges were observed in these silty waters.

In this preliminary work it soon became apparent that for every situation where CP light improved contrast, another situation would arise where it degraded contrast. Contrast improvement appeared to be conditionally dependent on the types, sizes, and concentrations of scatterers in the water. The world ocean has many waters which contain different scattering conditions. Because of this it was thought

that a controlled laboratory investigation of CP light contrast improvement would aid more in determining limits of usefulness, i.e., scatterer size and concentration, than would a few more expensive shipboard experiments.

3. Purpose of Present Work

The purpose of this report is twofold:

a. To describe an optical engineering study involving laboratory contrast measurements, and

b. To estimate from the laboratory study regions of the ocean where circular polarization might aid underwater visibility.

In order to predict the usefulness of increasing visibility by improving contrast with circular polarization it was necessary to compare unpolarized lighting with CP light in the laboratory under a variety of controlled scattering conditions. The size and concentration ranges of the scatterers used in the laboratory were chosen to duplicate the ranges of natural scatterers as determined by a literature search. While current chemical technology can supply a collection of well determined sizes covering the range of natural scatterers, there is no similar choice of refractive indices. The relative refractive index of the experimental spherical scatterers was m = 1.20, a value near the upper limit of refractive indices for marine scatterers.

An estimation was made of the effectiveness of CP

light for contrast improvement in different ecological regions of the ocean. The literature was searched concerning the mechanisms of light transmission, absorption, and scattering in the ocean. Specific information including the types, sizes, refractive indices, and probable location of particles was gathered. This was combined with the laboratory work to qualitatively predic, possible areas of CP light contrast improvement in the oceans.

CIRCULAR POLARIZATION FOR IMPROVING UNDERWATER VISIBILITY

Chapter Two

1. Description and Production of Circularly Polarized Light

Circularly polarized light is an optical wave in which an electric vector of constant amplitude rotates about the direction of propagation at the optical radiation frequency (2). By optical convention, if the direction of rotation appears clockwise to an observer looking into the direction from which the light is propagated, the light is called right-handedly circularly polarized; if counterclockwise left-handedly circularly polarized. In practice, polarized polychromatic light may be made into "quasi"-circularly polarized light with a commercial circular polarizing filter, i.e., a dichroic linear polarizer cemented to a commercial $\frac{1}{4}$ wave retarder at an angle of 45° between the orthogonal slow and fast axis of the retarder. The spectral region for which the retarder is a $\frac{1}{4}$ wave plate is $\lambda = 555\mu$ at the middle of the visible spectrum, for Polaroid Corporation HNCP 37 CP material.

The unpolarized polychromatic light upon passage through the dichroic polarizer becomes linearly polarized; one-half of this linear polarized light is projected onto

the fast axis and one-half onto the slow axis of the retarder. The slow axis light is retarded from the fast axis by $\frac{1}{4}$ wave, and the resultant polychromatic electric vector of the light leaving the retarder is circularly polarized.

When an observer views a circular polarizing filter from the cemented polarizer side if the retarder slow and fast axes have the positions shown in Fig. 3, the circular polarizer is right handed (RHCP); if as in Fig. 4, it is left handed (LHCP).

Fig. 3 RHCP

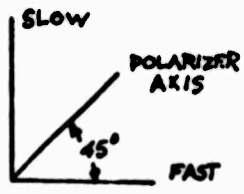

Fig. 4 LHCP

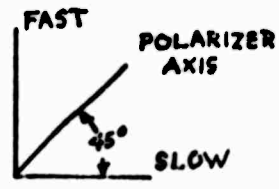

Circular polarizing filters have the property that only CP light of the same handedness as the filter will pass through the filter and light of the opposite handedness will be absorbed in the polarizer. It is this property that allows CP filters to be used to improve underwater visibility.

2. Application to U/W Contrast Improvement (Single Scatter Conditions)

With the circular polarization technique, an underwater target is illuminated by a source of right-handed (or left-handed) circularly polarized light located some distance from the target (Fig. 5). A receiver, with a right-handed (or left-handed) circular analyzer mounted at the

entrance pupil is located near the source and is used to "view" the target. Light from the source is scattered by particles in the medium into the receiver.

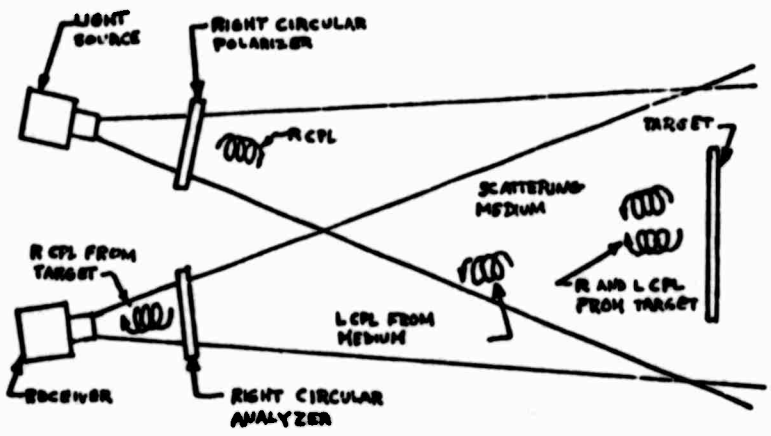

Fig. 5. Circular polarization for elimination of back-scatter.

For the following it will be assumed that mean diameter of the scattering particles will be much less than the distance between particles, i.e., single and not multiple scattering will dominate. Scattering particles in most ocean waters range in size from molecules with diameters much smaller than the wavelength of light to large organisms of diameters around 100μ (4, 13, 14). With respect to sea water, the relative refractive index range, m, of all but a very few material substances found in the ocean is $1.0 \leq m \leq 1.2$ (1). The particulate matter is non-absorbing. (A more detailed discussion of naturally occurring particulate matter will be given in Chapter Three.)

The right-handed CP light from the source travels through the water toward the target. Some of the photons encounter the particulate matter in the water and are scattered at the angles around 180° back into the receiver. The smallest particles in the water of diameter $d \ll \lambda$ will follow Rayleigh scattering theory and reradiate LHCP light into the receiver. The intermediate sized particles $d \sim \lambda$ will reradiate LHCP light according to Mie scattering theory. (Mie theory is rigorous only for spherical scatterers. However, much experimental work has shown that the theory holds for other scatterer geometries.) The large particles, $d \gg \lambda$, will follow the laws of geometrical optics. They scatter light back into the receiver by Fresnel reflection from the back outside surface or from the front inside surface of the particle after refraction (Fig. 6). The RHCP source photons will become LHCP light upon this reflection and travel back to the receiver. All of the RHCP photons scattered by these processes will now be LHCP entering the receiver.

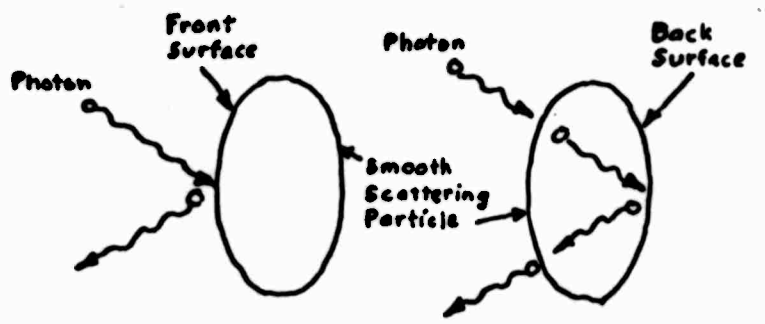

Fig. 6. Photons reflecting externally and internally from smooth scattering particles.

The photons reflected diffusely from the target will have their polarization changed. Reflection from the target may be either a surface or a volume effect depending upon the target material being a conductor or a dielectric. A conducting metallic surface will return RHCP light as LHCP light.

In general, most underwater objects that would serve as targets are coated with some sort of dielectric paint to resist marine corrosion. Therefore, the special case of a metallic reflecting surface will not be considered.

A dielectric painted target will both specularly and diffusely reflect photons. The specular reflections will change incident RHCP light to LHCP light. The diffuse reflections will be a combination of RH and LHCP light. A completely diffusing white Lambertian surface will cause the reflected light to be composed of equal amounts of RH and LHCP light and will appear unpolarized (2).

The resultant light flux reaching the receiver from the scattering particles is LHCP. The flux from the target is both RHCP and LHCP light. The receiver has a RHCP filter mounted at its entrance pupil so that the LHCP light from the scattering particles is filtered out and doesn't reach the receiver. The LHCP light from the target is also filtered. The only light that passes through the analyzer into the receiver is the RHCP light reflected from the target.

Without the polarizing filter on the receiver the luminance from the target is N_t consisting of RHCP and LHCP light; the luminance from the scatterers in the receiver's field of view is N_b, prevalently LHCP light. The ratio of target luminance to background luminance is N_t/N_b or apparent contrast is $C = (N_t/N_b) - 1$

With the RHCP filter on the receiver the target luminance is reduced to approximately 0.45 N_t because the LHCP is filtered out. The LHCP backscatter luminance will not pass through the RHCP filter into the receiver and will become very small, so that $N_b \rightarrow 0$.

Note that the apparent background luminance is the sum of the transmitted inherent ambient background luminance and the backscattered luminance from the source. For deep operations far from the photic zone or for night operations the ambient luminance may be negligibly small, and the background is all backscatter. Using dichroic type CP filters on source and receiver, the apparent background luminance N_b will be reduced to 0.15% of the unpolarized backscatter (calculated from ref. 20). Under these conditions the ratio of target luminance to background luminance is 300 times the ratio without the CP filters indicating a corresponding large increase in apparent contrast.

3. Extension to Double and Multiple Scattering Cases

The validity of the preceding explanation for the

reduction of backscatter with the CP light depends on the assumption of a predominance of single scattering. The value of the optical depth of the water may be used to indicate the prevalent type of scattering (26). Optical depth is defined as αr the product of α, the volume attenuation coefficient and r, the optical path length. If the optical depth has a value $\alpha r < 0.1$, then single scattering occurs; if $0.1 < \alpha r < 0.3$ double scattering and if $\alpha r > 0.3$ multiple scattering.

The effects of double scattering or multiple scattering upon polarization are not precisely know. However, some comments may be made concerning a probable precess by which backscattering will occur in double and multiple scattering media.

The scattering coefficient, $\sigma(\theta)$, is a differential volume scattering function related to S, the total scattering function. S is the amount of light leaving a collimated light beam by scattering per unit length of beam travel. $\sigma(\theta)$ is the angular differential of S with respect to solid angle, or

$$S = \int_0^{\pi} \int_0^{2\pi} \sigma(\theta) \sin\theta \, d\theta \, d\phi$$

(23,24,25).

Units of $\sigma(\theta)$ are ln/meter · steradian. $\sigma(\theta)$ may be further divided into a forward scattering function $f(\theta)$, $0 < \theta < 90^{\circ}$ and a backward scattering function $b(\theta)$, $90 < \theta < 180^{\circ}$.

The extreme angular dissymmetry of measured light

scattering coefficients $\sigma(\Theta)$ in natural waters indicates that most scattered light is forward ($0^{o} \leq \Theta < 90^{o}$) scattered by refraction and transmission through scattering particles and diffraction around particle edges (4). A much smaller percentage of light is backscattered $90^{o} < \Theta \leq 180^{o}$ by reflection.

For the double scattering an approximation to the scattering function may be easily obtained with the following qualitative argument. Note the scattering within $\pm 10^{o}$ of the forward beam direction accounts for 80% of the total scattering (17).

Now $f(\Theta)$ is the forward single scattering coefficient from $0^{o} < \Theta < 90^{o}$ and $b(\Theta)$ is the backward single scattering coefficient where $f(\Theta) >> b(\Theta)$. In a double scattering process the dominant process will be forward scattering within 10^{o} of the beam direction. The forward scattering coefficient will be roughly

$$f_2(\Theta) \sim f(\Theta)\ f(0^{o}) + b(\Theta)^2 \sim f(\Theta)\ f(0^{o}),$$

the result of two refractions and transmissions. The backscattering coefficient will be

$$b_2(\Theta) \sim b(\Theta)\ f(0^{o}) + f(0^{o})\ b(\Theta) = 2b(\Theta) f(0^{o}),$$

the result of a reflection and a refraction and transmission in either order.

Polarization is unchanged by refraction and transmission so that the double scattered photons returned to the receiver will have essentially the same polarization as a

singly scattered photon. Hence, reflected LHCP light would be unchanged after one refractive scatter. A similar argument may be applied to multiple scattering cases.

REVIEW OF UNDERWATER LIGHT ATTENUATION

Chapter Three

1. Analysis of Attenuation into Scattering and Absorption

The radiance N(r) in the field of a collimated light source is attenuated in the ocean according to the expression

$$N(r) = N(o)\, e^{-\alpha r} \quad ; (4)$$

N(o) is the inherent source radiance, r is the distance down beam where N(r) is measured and α is defined as the volume attenuation or extinction function (units of reciprical length).

The ocean consists of "pure" sea water and a composition of dissolved organic substances together with suspended organic and inorganic particulate material. Hence, the light attenuation coefficient may be expressed as

$$\alpha = \alpha_w + \alpha_s + \alpha_p$$

where α_w is attenuation due to the "pure" sea water.

α_s is attenuation due to the dissolved organic substances.

α_p is attenuation due to the particulate matter.

Any single attenuation coefficient may be further broken down into $\alpha_i = a_i + s_i$

where a_i is the effect of light absorption, i.e., a permanent loss of light by the conversion of light evergy into heat or some other energy form; and s_i is the scattering of light energy out of the collimated beam, simply a spatial redistribution of light flux.

For the "pure" water attenuation $\alpha_w = a_w + s_w$, Dietrich points our that the molecular absorption a_w has a much greater effect than s_w, the molecular scattering related to thermally caused spatial in homogenities in optical density (3). The scattering in the region is proportional to λ^{-4} i.e., Rayleigh scattering. Dietrich states: "....only in the spectral region of 380-500 mμ with the maximum at 460mμ is scattering in "pure" sea water of the same order of magnitude as absorption. For wavelengths greater than 580mμ, the contribution of scattering to extinction is less than 1%." For 680 mμ, s <1 o/oo α Duntley points out that in the very clearest blue ocean water the scattering by water molecules is only 7% of the total scattering coefficient (4).

The contribution to attenuation of the dissolved organic material is primarily in absorption, i.e., $\alpha_s = a_s$. This is the "yellow" substance which probably comes from decomposing phyto plankton (3,4,12). The effect of the "yellow" substance is to cause greater absorption of light at the shorter bluer wavelengths and hence to shift the "pure" sea water maximum at 460mμ toward the green part of the spectrum. Dietrich estimates that there is 3 to 10 times

as much dissolved organic material as live organisms in the ocean.

Particle contributions to volume attenuation are mostly scattering in nature. Tyler states that the absorption of naturally occurring organic particles can be ignored (23, 24). Burt quotes work by Ross and Kerr, 1931, to show that of the inorganic particles, only a very small fraction (no figures given) have absorptive indices large enough to have any appreciable effect on attenuation. Duntley states that the predominant scattering mechanism in the oceans are transparent organisms and other particles large compared to the wavelength of light.

Therefore, it may be assumed that the volume attenuation coefficient for natural ocean waters may be written as

$$\alpha = a_{w+s} + s_p$$

to a very close approximation for the visible spectral region, where again almost all scattering is caused by suspended particulate matter.

Ranges of values for the spectral volume attenuation coefficient, α_λ, encountered in natural waters are given by Hulbert, Fig. 7. This data is for distilled, coastal, and bay waters (12). Figures 8 and 9 are spectral attenuation coefficients measured by R. Hughes in waters of the California current off San Clemente Island (11). Figure 10 is a composite plot of spectral volume attenuation for

λ= 498.0 mμ versus depth in meters for various waters of the Northern Pacific Ocean. This data was taken by the author with the Naval Weapons Center Null Balance Transmissometer (8,9).

Typical limits of α for the spectral region from 450 mμ to 550 mμ are from $0.10<\alpha<0.53$ (ln/meter) for surface waters to 50 to 100 meters depth; and from $0.05<\alpha<0.10$ (ln/meter) for waters below 100 meters. As an indication of an upper limit for turbid waters, a measurement of attenuation for λ= 498.0 mμ performed at the NUWC Morris Dam fresh water test facility yielded an α= 4.0 ln/meter.

2. Turbidity and Naturally Occurring Scatterers

According to Dietrich and other sources (3, 13), turbidity is called "seston" and consists of three basic components:

(a) Mineral (minerogenic) turbidity caused by the salty runoff of rivers, from the grinding wave and tidal action against the shores and shallow coastal bottom, and from deep currents scouring the ocean bottom.

(b) Detritus - the organic and inorganic residue formed by the decomposition of organisms; this residue can range from the shards of diatomaceous glass shells to organic colloids.

(c) Living organisms - Nanno-, meso-, and macro plankton, mostly phyto-plankton (vegetables),diatoms, bac-

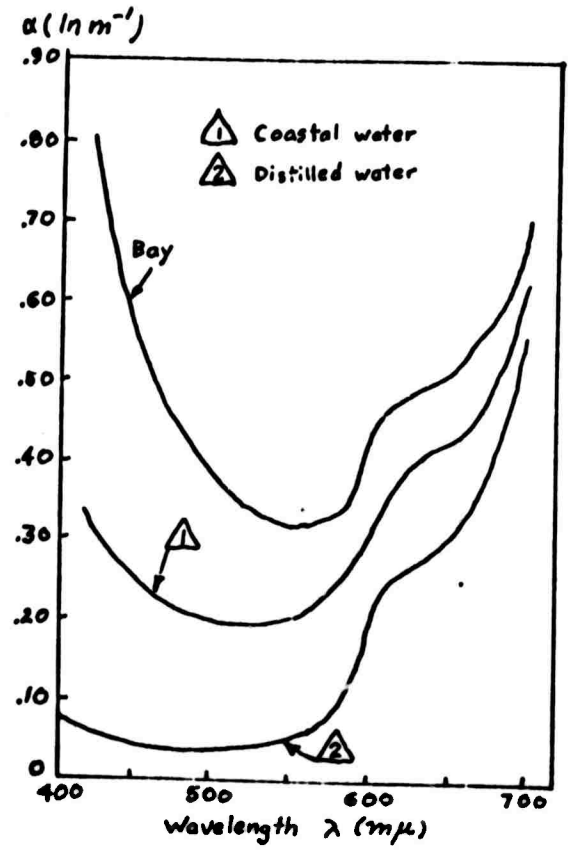

Fig. 7. Variation of α with wavelength in distilled, coastal, and bay waters.

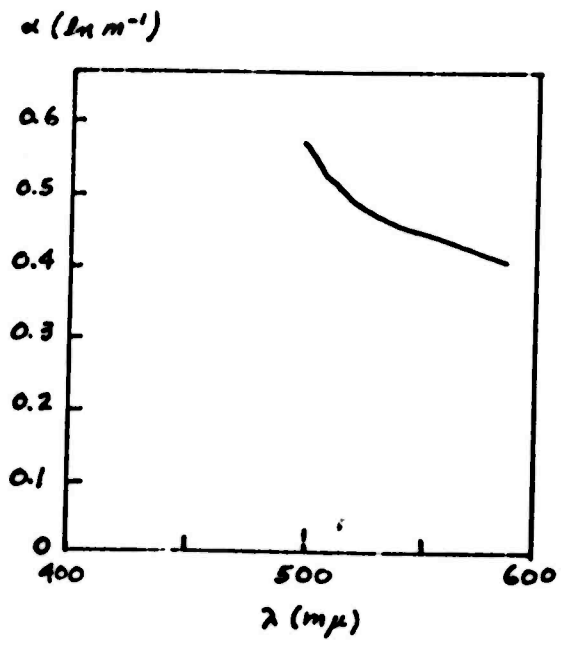

Fig. 8. Maximum alpha (minimum percent transmission) Vs wavelength at 40-meter depth.

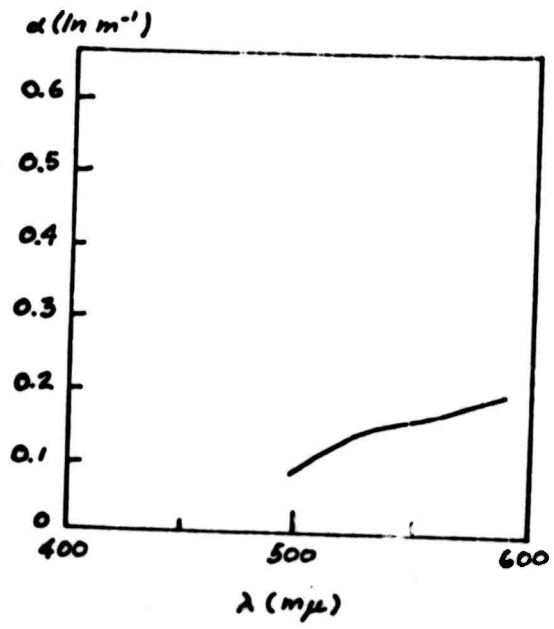

Fig. 9. Alpha Vs wavelength at depth of 300 meters.

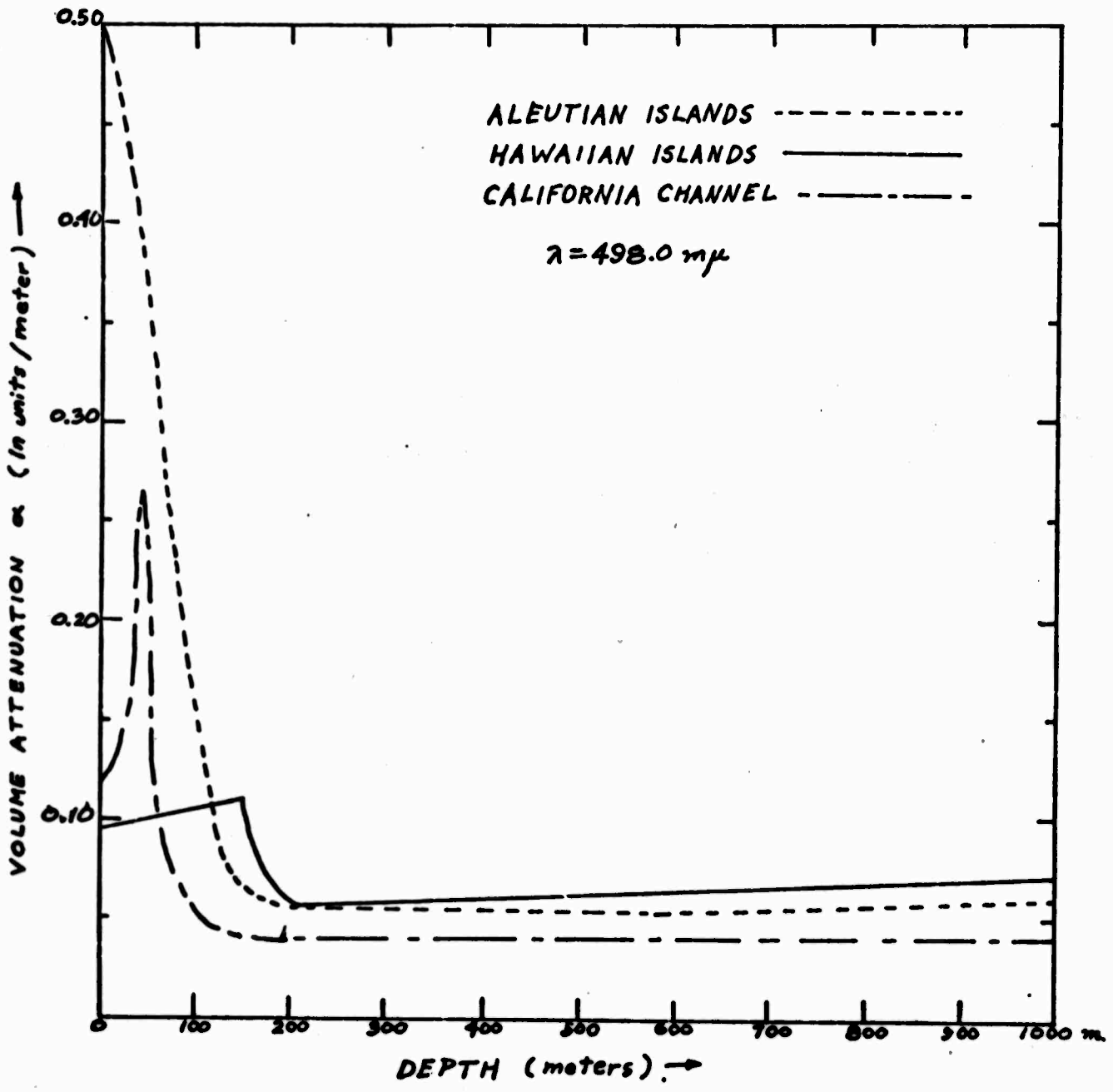

Fig. 10 Typical Attenuation Versus Depth

teria, dinoflagellates and other plant life plus a smaller contribution of zoo-plankton.

Mineral turbidity is a very important contributor to seston near land. On the Swedish Deep Sea Expedition 1947 - 1948, Jerlov reports that the larger sized mineral debris from the Nile flocculated and settled rapidly such that the surface waters 10 - 20 miles from the river mouth would barely show the effects of Nile runoff. Surface waters in the Red Sea contained fine sand blown by the wind from the surrounding land mass. This sand did not remain at the surface but quickly sank. Surface waters in the Panama Gulf contained considerable material from the nearby land. Jerlov points out that an abundance of terrogenious material here correlated with a general rich supply of nutrients and a corresponding large concentration of living organisms (9). On the other hand, a complete lack of terrogenious material in the South Central Pacific ocean correlated with a complete lack of surface organisms. No estimation of particle size was given other than that sizes of minute particles found in diatomoceous bottom oozes had median diameters of 7 - 8μ and 1μ in red clay. For predominately minerogenic particle data taken at Borno Station, 16 June 1953, Jerlov reports a preponderant number of particles of diameter near 1μ. However, the fractional contribution of these particles to the total cross-sectional area of suspended material was not important (14). Burt reports for Chesapeake Bay water, that the

particle diameter distribution was heavily skewed toward particles of diameter 1μ. In the same report, the relative refractive indices of common mineral solids, quartz, calcite, clay, are listed as ranging between 1.11 to 1.21 (1).

Living organic material is the chief contributor to seston in the surface waters or photic zone of the open ocean. Jerlov reports large concentrations of organisms found where deep upwelling equatorial currents diverge at the surface. The mean size of the organisms increases with the amount of available nutrients. Again the largest number of particles are found in the smallest diameters $\leq 1\mu$ range. These include bacteria, diatoms, dinoflagellates, and some algae. However, Jerlov quotes work by Goldberg, Baker, and Fox 1952, from which it is determined that the large numbers of plankton with sizes $<2\mu$ contribute less than 1% of the total surface of plankton (14). Tolbert mentioned similar figures (22). Burt reports work by Bennett (1951) that organic matter, both detritus and living, has refractive indices relative to water ranging from a low of 1.0 for very watery bacteria to a high $m = 1.2$ for tooth material. Cellulose, starch, muscle fiber, bone, some hemoglobin and protein fibers have refractive indices around $m = 1.15$ (1).

The detritus, decomposing organic particulate matter, settles out of the euphotic zone. According to Duntley, concentrations of detritus are found just above the thermocline (4). Jerlov points out that the detritus gradually

sinks out of this region on its journey to the bottom. Temperature and water density changes determine the sinking rate. Jerlov notes that large particles sink rapidly while smaller particles may remain suspended for years, and states "..... small particles - though not smaller than one micron - play the greater part of the suspended material in deep water." As has been previously mentioned, the refractive indices range of the detritus will be the same as the components of the living organisms.

EXPERIMENTAL WORK

Chapter Four

1. Overview

Measurements were made of the luminous flux returns from a black and white target placed in a glass tank filled with distilled water. Contrast degradation was observed as known amounts of small polystyrene latex spheres were added to the distilled water. The target was illuminated by a circularly polarized tungsten lamp projector, and viewed with a telescopic photometer on which a removeable circularly polarizing analyzing filter was affixed. Circularly polarized light is indistinguishable from natural unpolarized light unless viewed with a circular analyzer of opposite handedness. The target was first viewed directly without the filter on the photometer and measurements taken; the circular polarizing analyzer was then placed at the photometers entrance pupil and the measurements again made.

The monodisperse polystyrene latex balls placed in suspension in the water were from the Dow Chemical Company, Midland, Michigan. Six discrete monodisperse sized balls were used. Table I gives the means and standard deviations of the diameters of the particles used for each sample as measured by the company.

T A B L E I

Particle Mean Diameter (μ)	Std. Deviation
0.126	0.0043
0.234	0.0026
0.357	0.0056
0.557	0.0108
0.796	0.0083
1.099	0.0059

Three polydisperse distributions of styrene divinyl-benzene copolymer latex were used to simulate the larger ocean particles. The size distributions were 6-14μ, 25-55μ, and 50-100μ. The net result was that the effects on apparent target contrast of the black and the white target against the black velvet background were determined as a funtion of scattering particle diameter and concentration. This was done for both the ordinary unpolarized illuminator and for the circularly polarized illuminator and receiver.

Raw data was collected in the form of target and background luminance (ft. lamberts) versus concentration (ml.) of scattering solution present in the glass tank. The concentrations were converted to attenuation coefficients by an application of scattering efficiency formulas given by Van de Hulst (26). Seven measurements were made of the volume attenuation coefficient in the tank for light of wavelength λ= 542 mμ. This was done at the beginning of each run before any spheres were added to the distilled water and at the end when the concentration of spheres was a maximum.

These measured attenuation coefficients were compared with the attenuation coefficients derived from the known concentrations and approximate Mie scattering theory for light of $\lambda = 555\ m\mu$.

The apparent contrasts were calculated according to the expression

$$C = \frac{N_t - N_b}{N_b}$$

where C is the contrast of target at the calculated attenuation coefficient α, when the state of polarization is unpolarized or circularly polarized. The luminances N_t, N_b refer respectively to the measured target and background flux at attenuation α. The ratio of the CP contrast to the unpolarized contrast $R = \frac{C'}{C}$ was calculated and plotted versus attenuation coefficient for each scatterer size distribution. R was also plotted versus scatterer size for selected values of attenuation coefficient. By these ratios a comparison was made.

For the measurements the concentrations were such that many data points were taken in the attenuation coefficient range from $0.0 < \alpha < 1.0$ ln/meter. The particles used were in six monodisperse diameter distributions from 0.126μ to 1.099μ, and in three polydisperse diameter distributions of $6\text{-}14\mu$, $25\text{-}55\mu$, and $50\text{-}100\mu$ respectively. Both the attenuation coefficients and particles were of the order encountered in the ocean as listed in Chapter Three.

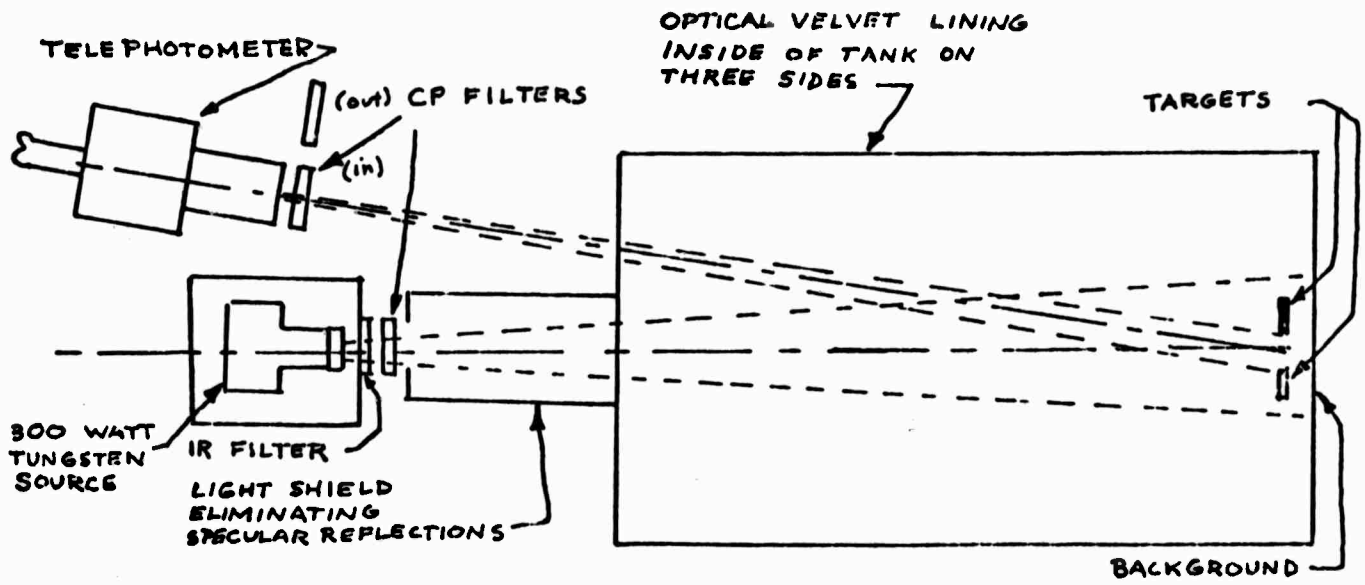

Fig. 11. Contrast Measuring Apparatus

2. Apparatus

Figure 11 is a schematic of the laboratory apparatus. The tank was a 60 cm length x 30.5 cm width x 25 cm height glass aquarium. When measurements were in progress black optical velvet was covered fastened to the inside sides and end glass of the tank. This greatly reduced the internal specular reflections in the tank.

Spectral attenuation coefficients (λ = 542mμ) for the distilled water without scatterers was measured and found to range from 0.10 ln/meter to 0.39 ln/meter.

The tank was filled with distilled water from 5 gallon bottles, filtered through a commercial Filter Corporation Fulflo 1μ filter. Air bubbles that clung to the sides

and to the target were stirred away. Fifteen to twenty minutes was allowed for any smaller bubbles that may have been introduced during filling to surface and disappear. The height of the water in the tank was measured with a scale and recorded.

A target, consisting of two 5" x 3/8" strips cut from 1/16" aluminum sheet and fastened upright to a 4" piece of heavy aluminum serving as base, was placed at the far end of the tank. One strip was painted a flat white and the other a flat black with government issue paint. The strips were mounted on the base so that they were separated from one another by $\frac{1}{4}$". This was done to decouple the aura effects caused by small angle forward scattering of the white target from the black target.

One set of Stokes parameter measurements were made to find the polarization of the light reflected from the targets and background in the water filled tank when illuminated by the quasi-circularly polarized tungsten projector lamp. Stokes parameters are well documented in optics texts (2, 18). The measurements were performed using Polaroid Corporation HNCP37 Circular Polaroid as an analyzer and retarder and the Model 2000 Gamma-Scientific Telephotometer.

The general state of polarized light is that of elliptical polarization. Any elliptical polarization can be further analyzed into linearly polarized and circularly

polarized components. This was done and it was found that the white target immersed in the water acted as a Lambertian diffuse surface. The light from this target was only 5.1% polarized and the circularly polarized component was 2.6% of the light. The light from the background was composed of the flux reflected from the optical velvet and any space lighting from backscatter in the water. This light was 35.5% polarized indicating that most of the flux came from the suspended material in the water. Of the polarized flux, 55.2% was circularly polarized.

The reflectivities of the targets were determined to be relative to the white target,

white	=	100.0%
black	=	3.3%
background	=	1.14%

An ordinary slide projector with a 300 watt tungsten bulb and an 125mm focal length f/3.6 projector lens served as light source. The projector was mounted on a small optical bench, together with a 2" x 2" heat absorbing glass and a 2" x 2" Polaroid Corporation HNCP37 circular polarization filter. It evenly illuminated the targets through the end window of the tank. To eliminate the reflections from the glass ends and sides of the aquarium the source and filters were completely enclosed in a flat black-painted cardboard housing that was butted tightly against

the end of the aquarium. It was very important that no specular reflections from this window were seen by the telephotometer because RHCP light becomes LHCP upon specular reflection from this window and behaves exactly like that scattered from a Rayleigh scattering medium. A RHCP filter on the receiver would gate this light out and give a considerable contrast improvement even if there were no backscatter in the water.

A Model 2000 Gamma-Scientific Corporation telescopic photometer was placed as near the axis of the light source as possible and measured the light flux from the targets and the water background. The photometer looked at light backscattered from the water in the angular range of 161° to 172° measured from the forward axis of the projector beam. The photometer is corrected with a photoptic filter such that its response is within a few percent of the visibility function, V_λ, of the human eye. The instrument has an internal calibration lamp such that all measurements were taken in photometric foot lambert units. A 6' angular field of view was used for the target measurements. The 6' field stop minimized any edge convolution effects while retaining enough sensitivity to record the returns from the low reflectivity background.

A removable circularly polarizing analyzer was mounted in the field of the telephotometer's collection optics by attaching a filter holder to the photometer's

light shield. Polaroid Corporation HNCP 37 circular polarizing sheet material was used both to circularly polarize the light source and to analyze the light signal at the photometer.

The effective combined spectral distribution, $T_\lambda V_\lambda$, of the tungsten lamp, T_λ, and the visibility function response of the Y-Scientific photometer V_λ was computed and is shown in Fig. 12. An approximate temperature of 3000°K for lamps of this type was found by use of tables of tungsten characteristics in reference 10. A spectral distribution for a tungsten source of 3000°K temperature was taken from a graph in reference 16. The visibility function was listed in reference 15.

The combined curve $T_\lambda V_\lambda$ has its maximum at λ=560mμ. The shape of the curve will be modified only slightly by passage through the short water path in the tank. The luminous power for the experiment is the total area under the curve.

The HNCP37 circular polarizers used in the source and receiver were manufactured by the Polaroid Corporation. As described by Polaroid: "A circular polarizer (CP) consists of a linearly polarizing filter and a $\frac{1}{4}$ wave retarding element whose slow and fast axis are at 45° to the axis of the polarizing filter." The retarder in the HNCP37 is of the "chromatic" type. That is, the retardation is only $\frac{1}{4}$ wave for light at wavelength λ = 560mμ ± 5mμ and the HNCP37

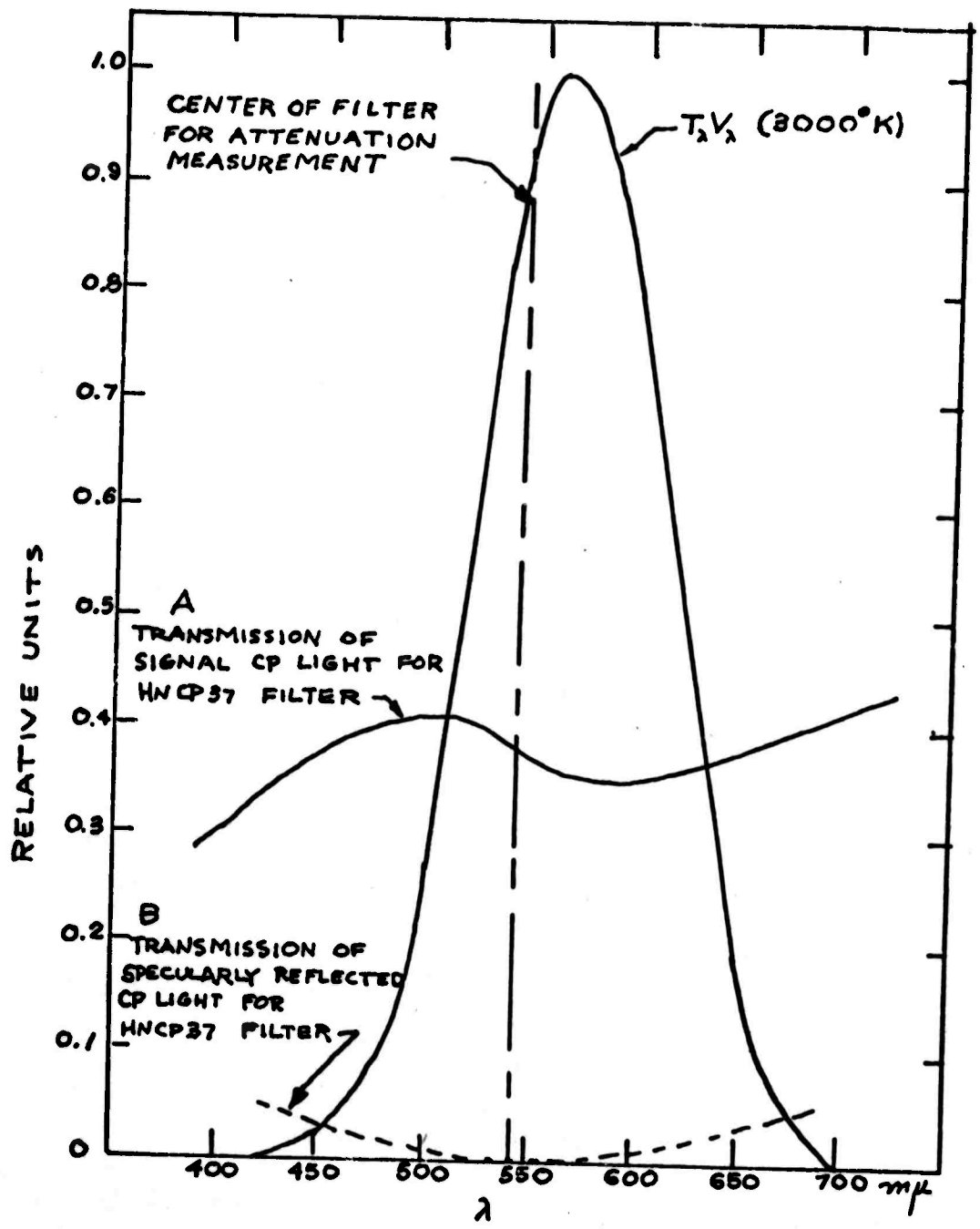
1.0
0.9
0.8
0.7
0.6
0.5
0.4
0.3
0.2
0.1
0
RELATIVE UNITS
CENTER OF FILTER FOR ATTENUATION MEASUREMENT
$T_\lambda V_\lambda$ (3000°K)
A
TRANSMISSION OF SIGNAL CP LIGHT FOR HNCP37 FILTER
B
TRANSMISSION OF SPECULARLY REFLECTED CP LIGHT FOR HNCP37 FILTER
400
450
500
550
600
650
700 mμ
λ

Fig. 12

only acts as a good circular polarizer at this wavelength. This wavelength is conveniently at the center of the $T_\lambda V_\lambda$ curve (Fig. 12). Figure 12 includes a Polaroid Corporation graph showing the spectral transmission of the CP material in curve A, and the opposite handedness circular polarization rejection properties in curve B. Curve B is plotted on the $T_\lambda V_\lambda$ graph showing its rejection properties for the light source--photometer spectral region used.

Because of the polychromatic nature of the 3000°K tungsten light source and the photometer, $T_\lambda V_\lambda$ (Fig. 12), it is seen that a small portion of the light in the "wings" of $T_\lambda V_\lambda$ was elliptically polarized. This elliptically polarized light would have its handedness reversed by a single reflection from a particle but would not be perfectly gated out by the circular analyzer on the receiver. Hence, elliptically polarized light from the "wings" filtered through into the receiver and caused contrast improvement to slightly degrade. The HNCP37 polarizing filters used were slightly inhomogeneous and had a preferred direction of orientation. Homogeneous CP filters have no such preference (20). For an arbitrary position of the respective polarization axes of the filters on the source and receiver, there was a noticable "violet" light leak of light reflected from specular surfaces or scattering particles. By visual observation it was found that this effect could be minimized if the CP filter on the source and the CP filter on the receiver were

oriented such that their respective polaroid axes were crossed.

3. Light Attenuation Measurements

For seven of the contrast measurements spectral volume attenuation coefficient measurements were taken in the tank of the filtered distilled water without scatterers. Volume attenuations coefficients were estimated for the rest of the contrast measurements by noting a linear correlation of the measured attenuations to the ratio of measured background flux to the flux from the white target with no scatterers added to the water. The general method of measuring α is mentioned by Duntley (4).

An apparatus schematic for the measurement of α is pictured in the Fig. 13. A diffuse light source consisting of a 7" x 7" x 7" box containing two 100-watt tungsten filament bulbs with a 5" x 5" frosted glass window was placed at the rear of the tank. The lamp output was periodically checked and found to be constant in time. Optical velvet lined the two sides of the tank to cut down internal specular reflection. An Optics Technology 2" x 2" dielectric-coated interference filter was affixed to the frosted glass window with black optical tape. The rest of the frosted glass was blacked out. The filter had a transmission maximum at $\lambda = 542m\mu$ with one half transmission points located at $\pm 6m\mu$ from the center wavelength respectively. The filter

converted the source into a source of diffuse spectral light flux of the interference filter wavelength.

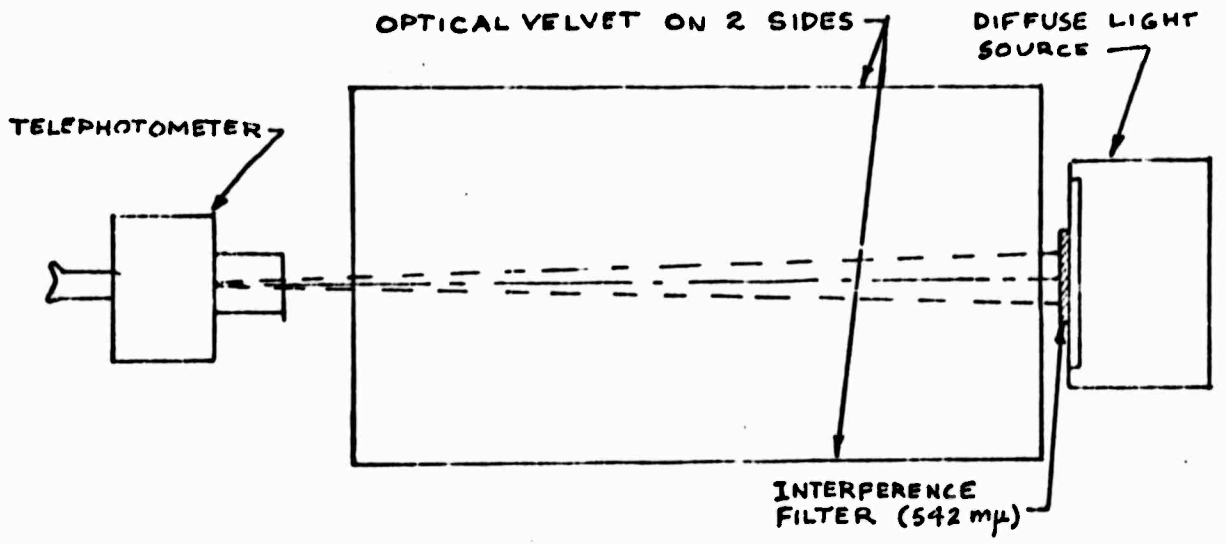

Fig. 13. Attenuation coefficient measuring apparatus.

The telephotometer with the 6' field looked normally through both end windows at the spectral source. Two measurements were made, one with the tank empty and one with the tank filled with the distilled water. Volume attenuation was derived as follows for one spectral source: N_o is the inherent spectral source radiance. With the tank empty the photometer looks at the source and measures radiance $N_1 = N_o T_{ag}^4$ where $(T_{ag})^4$ is the transmission of four air-glass interfaces. With the tank filled the photometer is focused on the source and measures radiance

$$N_2 = N_o T_{ag}^2 T_{gw}^2 e^{-\alpha r}$$

where T_{gw}^2 is the transmission of two glass-water interfaces

and r is the light path through water, i.e., the tank length in meters. The spectral attenuation is then

$$\alpha = -\frac{1}{r}\left(\ln \frac{N_2}{N_1} + 2 \ln \frac{T_{ag}}{T_{gw}}\right)$$

$T_{ag} = 0.960$ and $T_{gw} = 0.9964$ are calculated from the Fresnel reflection formula, assuming refractive indices of air $m_a = 1.0$, water $m_w = 1.33$, glass $m_g = 1.5$ (27).

Measurements of α were also made at the end of each run, when the scattering concentration was at a maximum. These measurements were compared with attenuation coefficients calculated from known particle concentration and scattering theory. This will be shown later.

The range of the attenuation coefficients for the distilled water without scatterers was $0.107 \leq \alpha \leq 0.3891$ ln/meter. Ideally for very clear water with negligible scattering, the contrast of a target illuminated with natural unpolarized light should equal the contrast as measured for circularly polarized illumination. As scattering increases with a corresponding increase in attenuation, the ratio of the contrast for the CP target to the unpolarized target will become greater. It was found that the initial CP to unpolarized contrast ratio measured with no scatterers placed in the water varied directly as the measured attenuation coefficient. As the measured extinction coefficient increased the improvement in contrast increased indicating that circular polarization was gating out light scattered

from unknown scatterers in the water. This effect was considered in the presentation of the contrast improvement computations to be given.

4. Calculation of Sphere Concentration and Attenuation Coefficients

All of the latex spheres received from Dow Chemical Corporation were in the form of 10% $\pm$ 0.01% by weight solids in distilled water solutions. For the monodisperse distributions the calculation of number concentration per unit volume was easily done. The density of bulk polystyrene is given as $\rho = 1.05$ gms/cm^3 (27). The initial mass concentration, M, (gms/cm^3) for the spheres as received from Dow Chemical was determined to be $M_b = 0.1005$ gms/cm^3. The mass of a single sphere of diameter, d (cm), is

$$M_1 = \frac{1}{6}\pi d^3\rho$$

and the number of spheres per cm^3 is

$$N_1 = \frac{M_b}{M_1} = \frac{0.1005}{(1.05)\left(\frac{\pi}{6} d3\right)} = \frac{0.1825}{d^3}$$

Typical concentrations are shown in the Table II.

T A B L E I I

$d(\mu)$	N_1 (# /cm^3)
0.1	1.825×10^{20}
1.0	1.825×10^{17}
100	1.825×10^{11}

This large number concentration was severely diluted in preparation of the test scattering solutions.

The number concentration calculation for the polydisperse distributions was more difficult. Dow Chemical could supply no other information than the 10% weight concentrations and the diameter limits on the polydisperse distributions, i.e., $6 \leq d \leq 14$, $25 \leq d \leq 55$, $50 \leq d \leq 100$. To perform the calculation of number concentration it was necessary to assume a size density distribution function $N(X)\,dx = N_o\,p(x)\,dx$. Three such approximation distributions, $p(x)\,dx$ assumed. These were a monodisperse distribution, a uniform distribution, and a Gaussion distribution. N_o was solved for in the same manner as for the monodisperse distributions. The number distribution of spheres was

$$N_o = \frac{M_b}{M_1} = \frac{M_b}{\rho \int_{d_1}^{d_2} p(x) \frac{\pi x^3}{6}\, dx}$$

where M_1 is the average mass of a single sphere.

then $N(x)\,dx = N_o\,p\,(x)\,dx$ where $N(x)$ is the number of spheres with diameter between x and $x+dx$. This will be further discussed in regard to the calculation of the attenuation coefficient.

A solution of monodisperse scatterers of known concentration was prepared by adding a measured volume of scattering material to a known volume of distilled water. Generally 0.5 milliliters of 10% scattering sclution was mixed with 99.5 milliliters of distilled water to form the

test solution. Chemical pipettes of 0.5 and 1.0 ml were used to draw the solution from the sample bottles. The accuracy of this method was very good, the error being the meniscus of the fluid in the pipette. Some difficulty was encountered in keeping the larger spheres (6-100μ) in suspension during a flux measurement. For these the procedure was to stir the solution with a glass rod and then quickly take a measurement.

The concentration in the test solutions made from the samples is then

$$N_2 = \frac{N_1 V_1}{V_1 + V_2}$$ for the monodisperse distribution; and

$$N_2(x)\,dx = N_0\, p(x)\,dx\, \frac{V_1}{V_1 + V_2}$$ for the polydisperse distribution.

V_1 is the total number of milliliters of solution taken from the sample bottle and V_2 is the number of milliliters of distilled water with which it was mixed. The final concentration of scatterers per cm^3 in the tank was then . . .

$$N_i = \frac{N_2\, \delta V_i}{V_3 + \delta V_i} \cong \frac{N_2\, \delta V_i}{V_3}$$

where V_3 is the aquarium volume of water, and δV_i is the total amount of test solution mixed in the tank at any time. V_3 was obtained using the measured height of the water when the tank was filled. Finally

$$N_i = \frac{(0.1825/d^3)\, V_1}{(V_1 + V_2)\, V_3}\, \delta V_i \pm 0.01\, N_i$$

a similar expression was derived for the polydisperse distributions.

In order to compare the data collected for various sizes spheres, it was necessary to convert the units of concentration for each sphere sample into the more universal units of the corresponding attenuation coefficient. The attenuation coefficient is a function not only of concentration but also of the projected area of a single sphere, and hence represents an obvious means of comparison for different sized distributions.

By definition the volume attenuation coefficient is given for a monodisperse distribution by

$$\alpha = N Q_{ext} (\pi d^2/4)$$

where again N is the concentration of spheres and $\pi d^2/4$ the projected area of a single sphere. The quantity Q_{ext} is an efficiency factor for a single sphere that is also a function of sphere diameter and the relative refractive index of the scattering sphere to that of the suspension medium.

For the polydisperse distribution, $N(x)dx = N_0 P(x)$ dx, the average volume attenuation coefficient is obtained from

$$\overline{\alpha} = \int_{d_1}^{d_2} N(x)\, Q_{ext}(x)\, \frac{\pi x^2}{4}\, dx$$

The efficiency factors, Q_{ext}, could be derived from rigorous Mie scattering theory. However, because of the difficulty involved in such a derivation, approximation theories covering three different size ranges were used instead (26). For the smallest sphere size, d= 0.126μ Raylcigh-Gans theory gave $Q_{ext} = |m-1|^2 \phi$ where m= 1.20 is the relative refractive

index of the bulk polystyrene and ϕ is a tabulated function of the diameter refractive index of water, and the spectral wavelength (26). The wavelength in air for which all efficiency factors were calculated was $\lambda = 555\ m\mu$, the center of the spectral $T_\lambda V_\lambda$ curve.

For the size range from $0.234\mu \leq d \leq 1.099\mu$, anamolous scattering theory supplied a functional expression for the efficiency,

$$Q_{ext} = 2 - 4\frac{\sin\rho}{\rho} + 4\frac{(1-\cos\rho)^2}{\rho^2}$$

The quantity ρ is a phase shift term and is given by

$$\rho = \frac{2\pi d}{\lambda}(m-1)$$

For the larger diameter polydisperse distributions use was made of the limiting condition from Mie theory that $\lim Q_{ext} = 2.0$. The largest error involved with this approximation was for $d = 6\mu$. The error here was ~15%. For the range 14μ - 100μ the maximum error was 1% deviation from rigorous Mie theory.

The attenuation coefficient for a concentration of monodisperse spheres was $\alpha = Q_{ext}(d)\frac{\pi d^2}{4}\frac{(0.1825/d^3)V_i}{(V_1+V_2)V_3}\delta V_i$ where the Q_{ext} is calculated from the approximation theory corresponding to the size d.

For the polydisperse distributions numerical calculations were made of the mean attenuation coefficient using all three of the assumed distributions $N(x)dx = N_0 p(x)dx$. The three assumed distributions were :

(a) Monodisperse $p(x)\,dx = \delta(x-\bar{x})\,dx \qquad \bar{x} = (x_1 + x_2)/2$

(b) Uniform $p(x)\,dx = \dfrac{dx}{x_2 - x_1}$ if $x_1 \le x \le x_2$

$= 0$ otherwise

(c) Gaussian

$$p(x)\,dx = \frac{1}{\sqrt{2\pi}\,\sigma} \exp\left(-\tfrac{1}{2}\left(\frac{x-\bar{x}}{\sigma}\right)^2\right) dx$$

where $\bar{x} = \dfrac{x_1 + x_2}{2}$ and $\sigma = (x_2 - x_1)/2$.

The volume attenuation was calculated in closed form

$$\bar{\alpha} = Q_{ext}\, N_0 \int_{d_1}^{d_2} p(x)\, \frac{\pi x^2}{4}\, dx \cdot \frac{V_1\, \delta V}{(V_1 + V_2)\, \bar{V}_3}$$

for the monodisperse and uniform distributions, and with Gaussian quadrature for the Gaussian distribution. N_0 was previously evaluated in a similar calculation. The maximum spread in α's calculated from the three assume d distributions was less than 5.4% for all three size ranges.

Table III is a comparison of the attenuation coefficients calculated from the above method for light of $\lambda = 555 m\mu$ with the attenuation coefficients measured for light of $\lambda = 542\ m\mu$.

The calculated volume attenuation coefficients, with the exception of the 0.126μ sphere derived from Rayleigh-Gans theory, are all larger than the corresponding measured attenuation coefficients. This is to be expected because of the finite field of view of the measuring photometer. In the theoretical calculation of the attenuation coefficient, light scattered at small forward angles leaves

TABLE III

Diameter	Measured α ln/meter	Calculated α ln/meter	% Difference
0.126	0.58	0.508	12.0
0.234	1.70	2.02	-18.7
0.357	2.72	3.12	-14.7
0.557	4.36	4.79	- 9.9
0.796	4.48	4.69	- 4.7
1.099	5.96	6.95	-16.6

the beam and is assumed distinguishable from the unscattered light. it is not "measured" by a theoretically infinitesimal detector. However, in real measurements the detector has a finite size and cannot distinguish small-angle forward scattered light from unscattered light. Hence, some scattered light will reach the photometer and the measured attenuation coefficients will be smaller than the theoretically calculated coefficients.

5. Results

Because of the low reflectivity and correspondingly small inherent contrasts of the black target for both polarized and unpolarized light, the data collected was deemed to be of little quantitative interest as the black targets merged into the background with only a little scattering material in the water. However, it was shown qualitatively that for the target there was little difference in contrast between the polarized and unpolarized lighting. Hence, the graphical data presented is only for

the white target.

The apparent contrasts, C, for each attenuation coefficient value and each polarization state were calculated from the definition

$$C = \frac{N_t - N_b}{N_b}$$

where N_t = target luminance

N_b = background luminance.

The inherent contrasts of the white target with no scatterers in the water differed depending upon whether the target was illuminated with the unpolarized light or with the CP light. When illuminated with the CP light, the inherent contrast was generally greater, ranging from 1.0 to 1.95 times the unpolarized inherent contrast. This was believed to be caused by the Rayleigh molecular scattering of the water and by small motes and dust particles remaining in the water in spite of the filtration system. To decouple this effect and to obtain a measure of the contrast improvement related only to the arbitrary size and concentration of latex scattering spheres in the tank at any time, it was necessary to normalize the measured apparent contrasts at attenuation α, $C(\alpha)$, by the measured inherent contrast, $C(o)$, at attenuation $\alpha = 0$ for the corresponding polarization state. Figures 14-22 are plots of the normalized contrasts versus the calculated attenuation coefficients, α, for a specific sphere size. The curves for the CP contrasts and the unpolarized

contrasts are appropriately labeled. On the plots for sphere sizes $0.126\mu \leq d \leq 1.099\mu$, the ratio of the circular polarized contrast to the unpolarized contrast is plotted with a dotted line. It may be seen that this ratio decreases with increasing sphere size and is just barely present for the 1.099μ spheres. The range $0 \leq \alpha \leq .70$ (ln/meter) is of the magnitude encountered in most of the ocean.

From these graphs it is easily seen that contrast is improved for the smaller diameter $d < 0.557\mu$ spheres at all concentrations, the improvement becoming more marked as the scatterer concentration and corresponding attenuation coefficient increase. The $d = 0.796\mu$ spheres show about a 20% contrast improvement ratio for all attenuations, while the $d = 1.099\mu$ show no improvement in contrast ratios. All of the contrast improvement ratios in the size ranges $6\text{-}14\mu$, $25\text{-}55\mu$, and $50\text{-}100\mu$ are less than 1.0, indicating a degradation in CP contrast.

Figure 23 is a plot showing the effectiveness of CP contrast improvement as a function of sphere size for various attenuations. It may be seen that for all sphere sizes and all attenuations in the range $0 < \alpha < 1.0$ ln/m contrast ratios increase with the exception of the 1.099μ sized spheres for $\alpha = 0.25$.

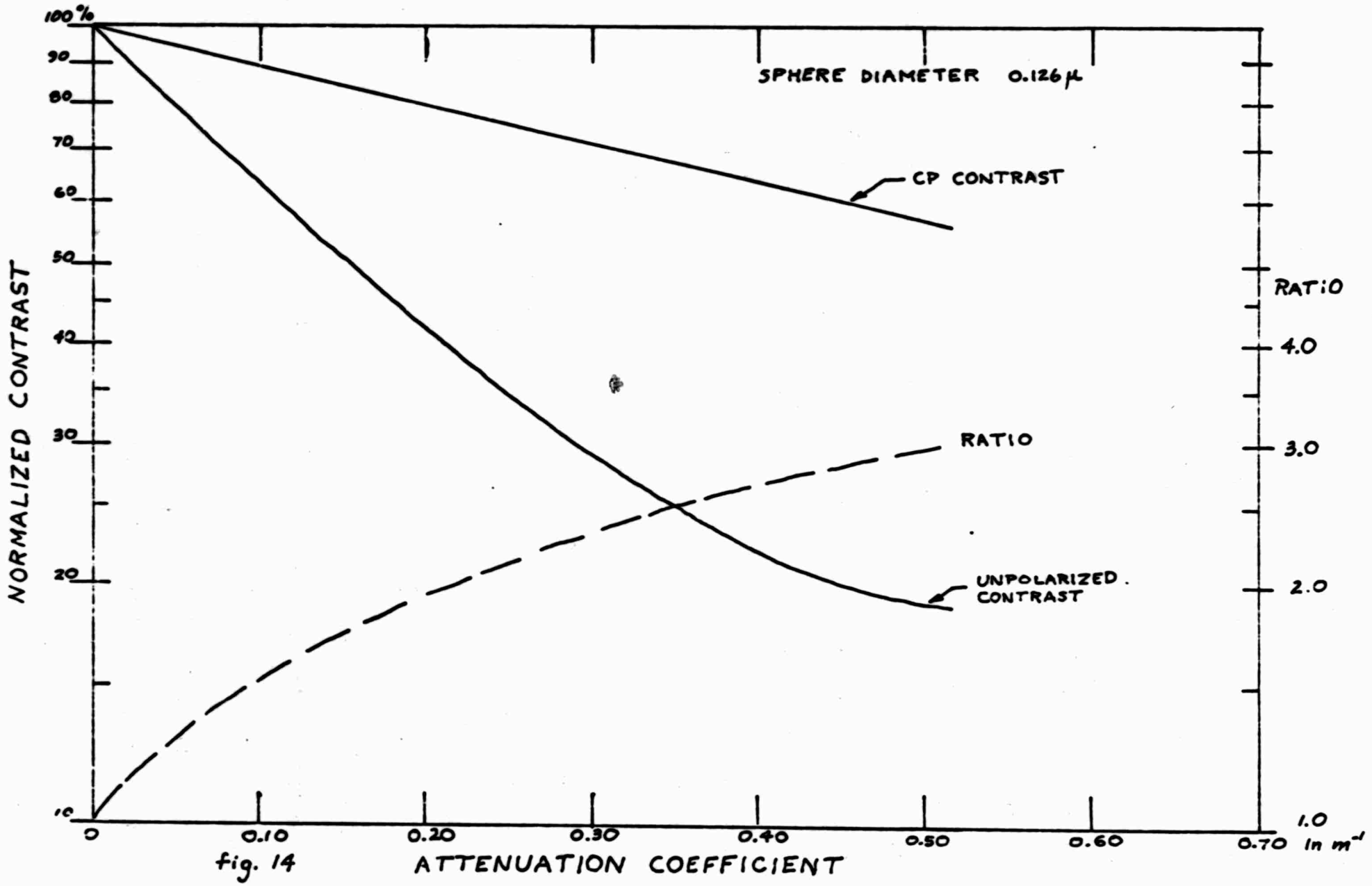
100%
90
80
70
60
50
40
30
20
10
NORMALIZED CONTRAST
SPHERE DIAMETER 0.126 μ
CP CONTRAST
RATIO
UNPOLARIZED CONTRAST
RATIO
4.0
3.0
2.0
1.0
0
0.10
0.20
0.30
0.40
0.50
0.60
0.70
ln m⁻¹
ATTENUATION COEFFICIENT

fig. 14

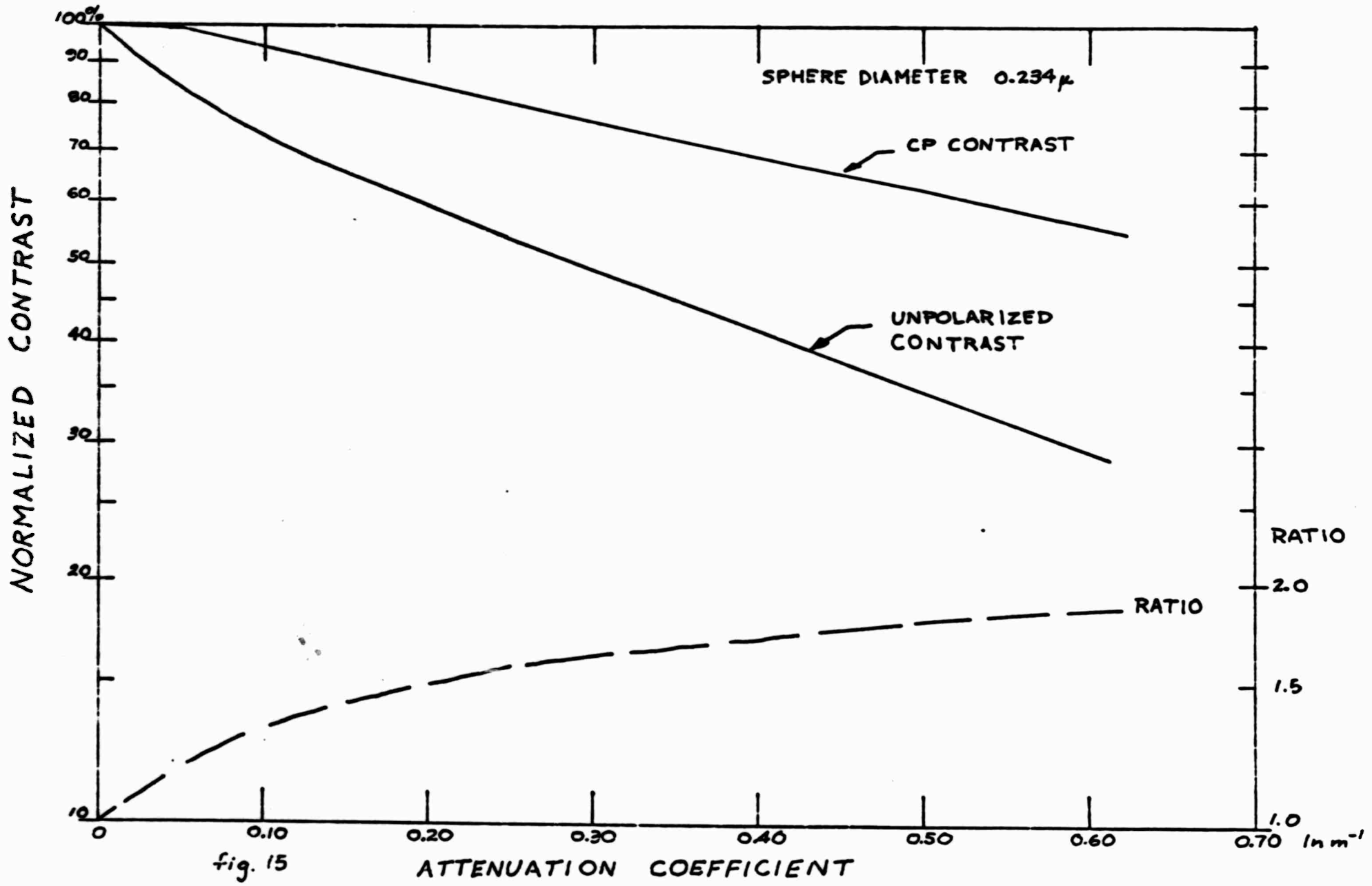
100%
90
80
70
60
50
40
30
20
10
NORMALIZED CONTRAST
SPHERE DIAMETER 0.234 μ
CP CONTRAST
UNPOLARIZED CONTRAST
RATIO
RATIO
2.0
1.5
1.0
0
0.10
0.20
0.30
0.40
0.50
0.60
0.70 ln m⁻¹
ATTENUATION COEFFICIENT

fig. 15

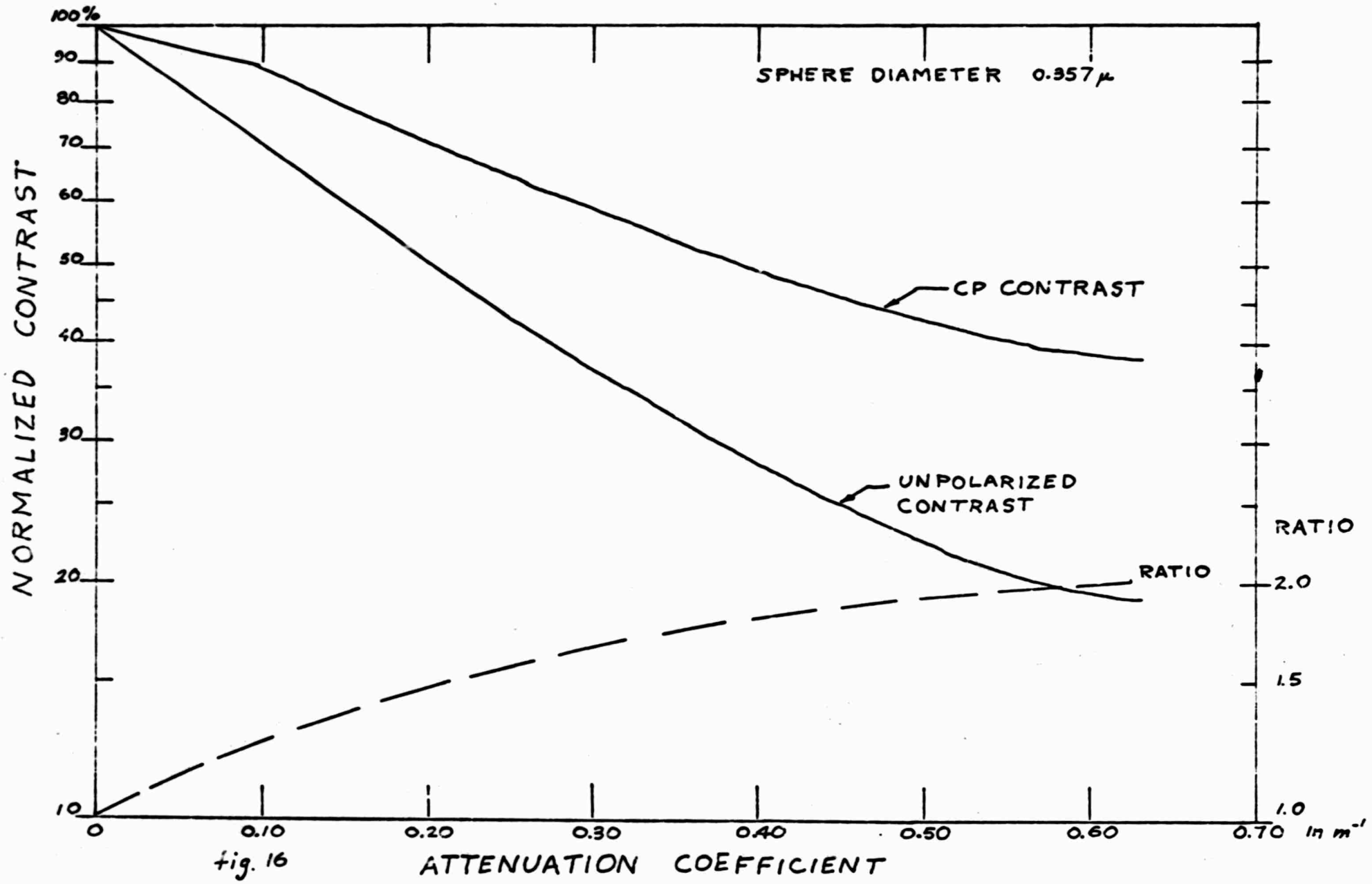
SPHERE DIAMETER 0.357μ
CP CONTRAST
UNPOLARIZED CONTRAST
RATIO
NORMALIZED CONTRAST
100%
90
80
70
60
50
40
30
20
10
2.0
1.5
1.0
0
0.10
0.20
0.30
0.40
0.50
0.60
0.70 in m⁻¹
ATTENUATION COEFFICIENT

fig. 16

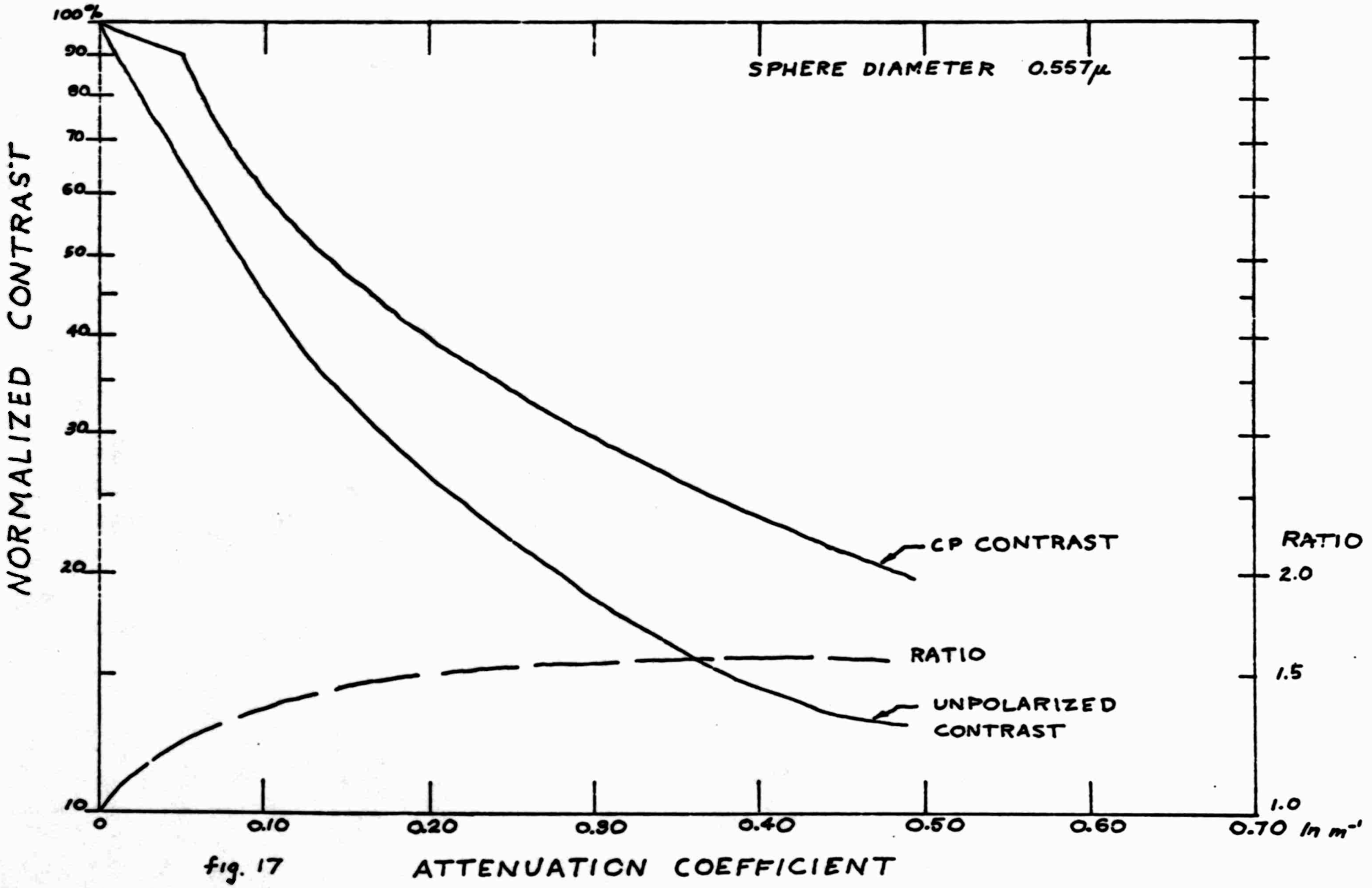
SPHERE DIAMETER 0.557μ
NORMALIZED CONTRAST
100%
90
80
70
60
50
40
30
20
10
CP CONTRAST
RATIO
UNPOLARIZED CONTRAST
RATIO
2.0
1.5
1.0
0
0.10
0.20
0.30
0.40
0.50
0.60
0.70 ln m⁻¹
ATTENUATION COEFFICIENT

fig. 17

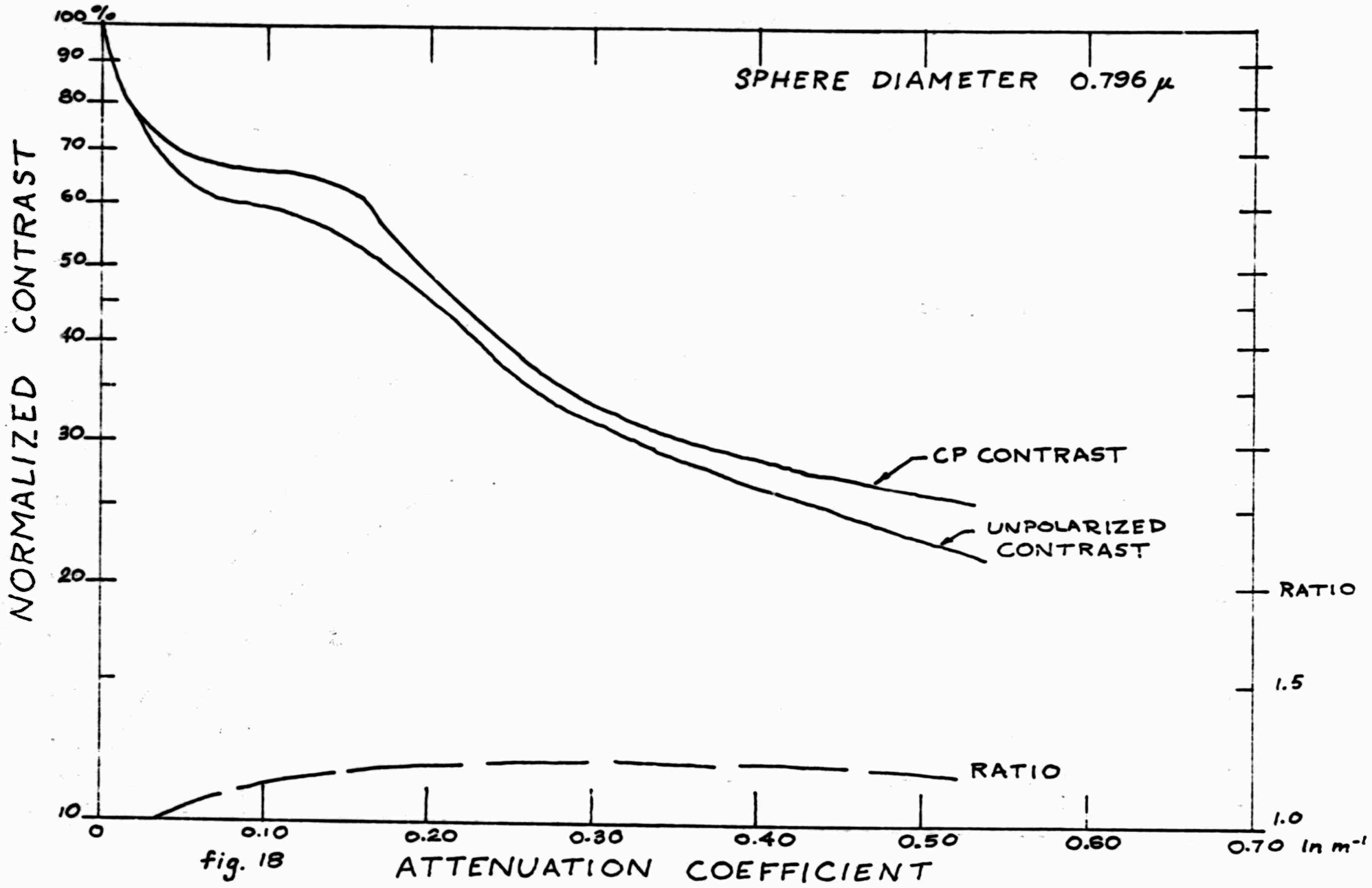
SPHERE DIAMETER 0.796 μ
NORMALIZED CONTRAST
100 %
90
80
70
60
50
40
30
20
10
CP CONTRAST
UNPOLARIZED CONTRAST
RATIO
RATIO
1.5
1.0
0
0.10
0.20
0.30
0.40
0.50
0.60
0.70 ln m⁻¹
ATTENUATION COEFFICIENT

fig. 18

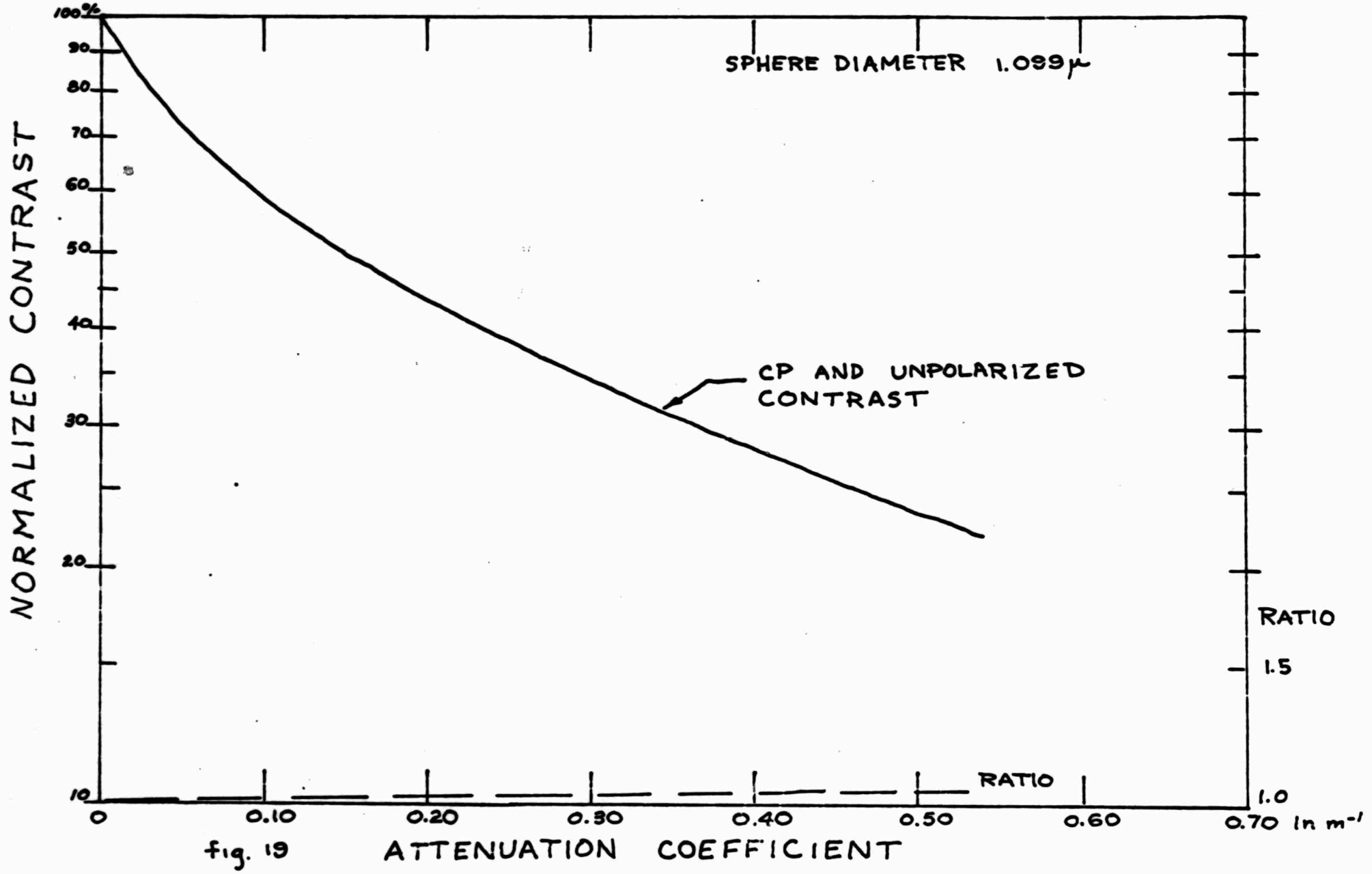
SPHERE DIAMETER 1.099μ
CP AND UNPOLARIZED CONTRAST
NORMALIZED CONTRAST
100%
90
80
70
60
50
40
30
20
10
RATIO
1.5
1.0
RATIO
0
0.10
0.20
0.30
0.40
0.50
0.60
0.70 ln m⁻¹
ATTENUATION COEFFICIENT

fig. 19

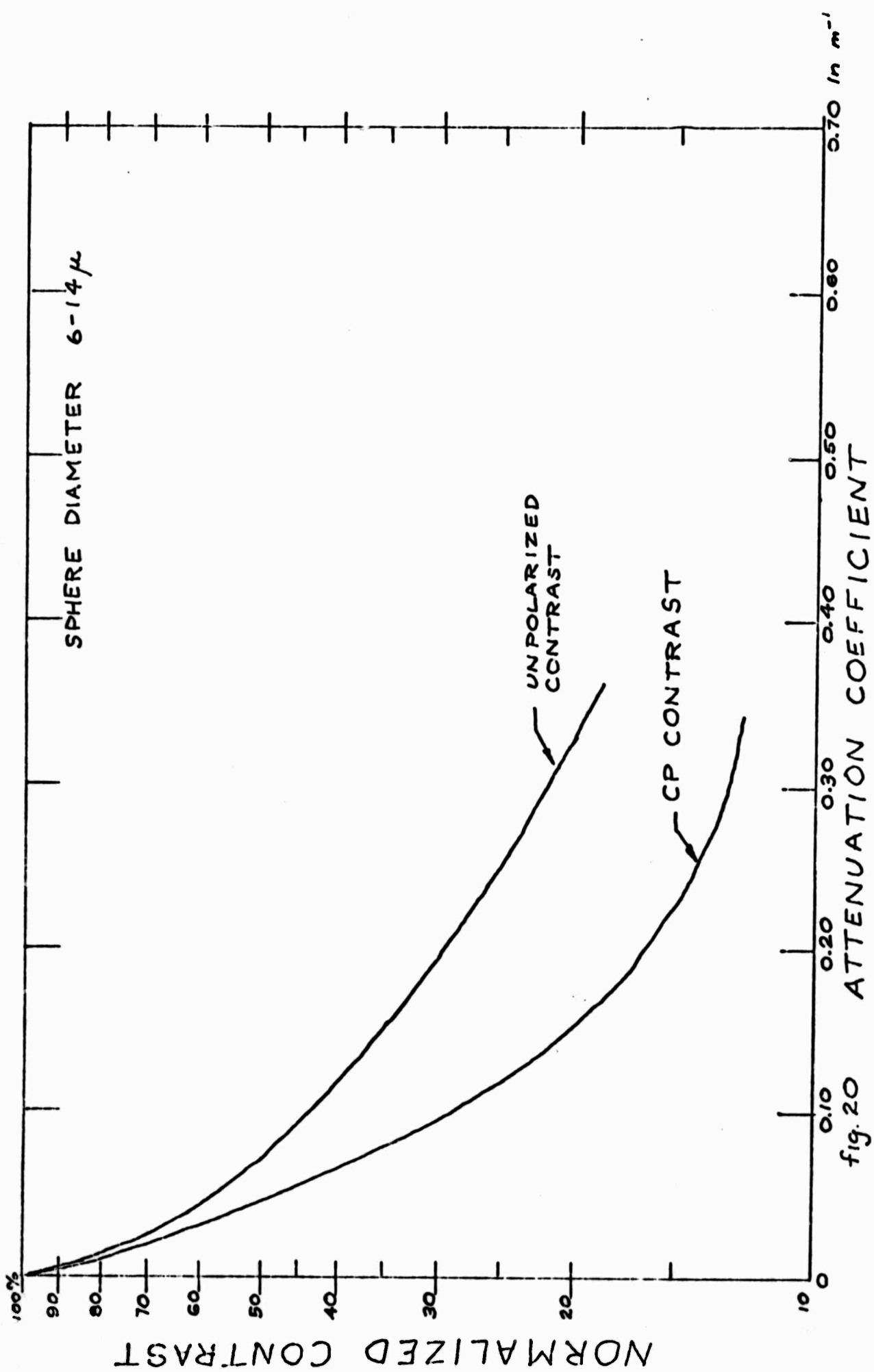
SPHERE DIAMETER 6-14μ
UNPOLARIZED CONTRAST
CP CONTRAST
NORMALIZED CONTRAST
100%
90
80
70
60
50
40
30
20
10
0
0.10
0.20
0.30
0.40
0.50
0.60
0.70 ln m⁻¹
ATTENUATION COEFFICIENT

fig. 20

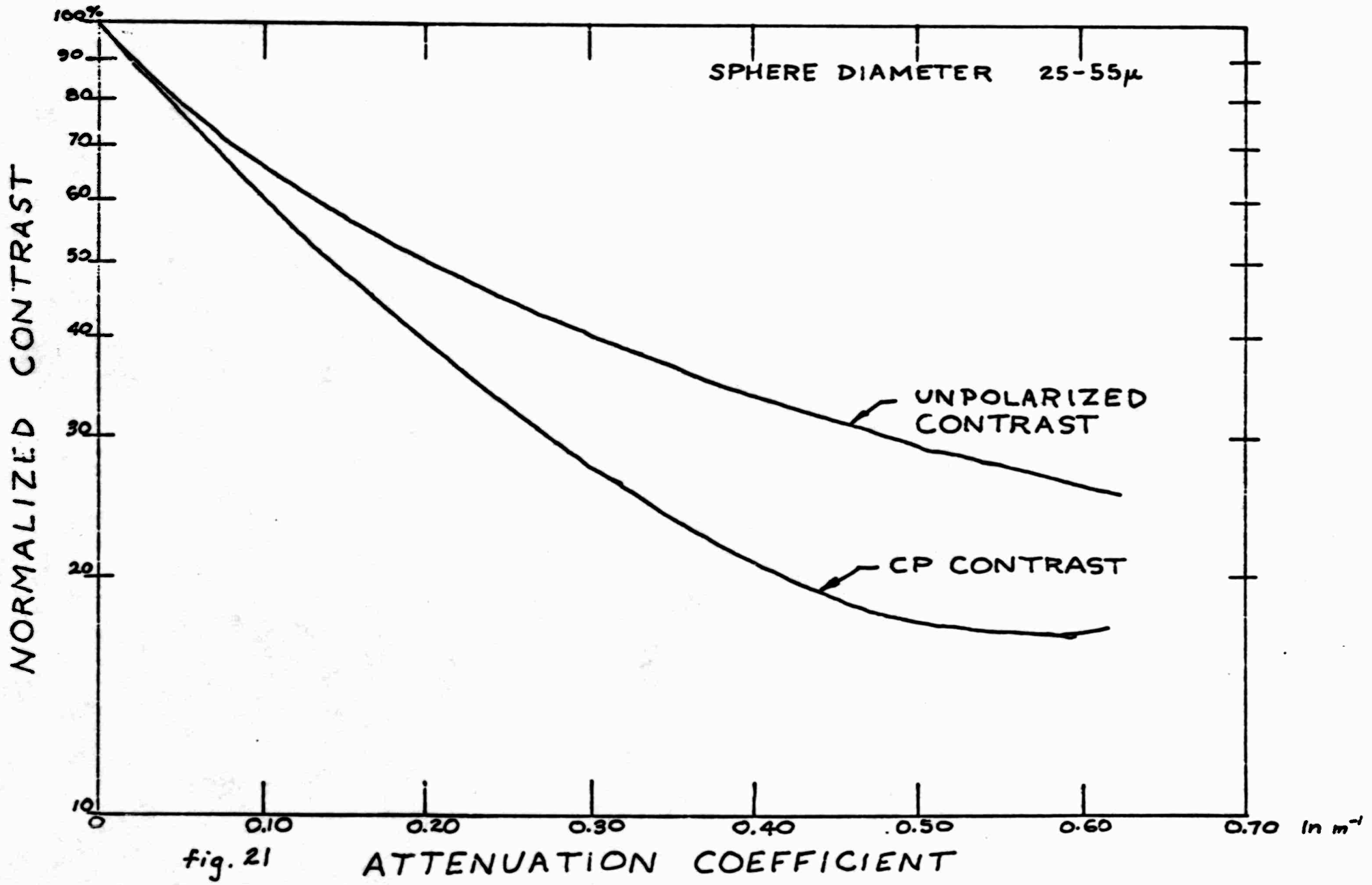
100%
90
80
70
60
50
40
30
20
10
NORMALIZED CONTRAST
SPHERE DIAMETER 25-55μ
UNPOLARIZED CONTRAST
CP CONTRAST
0
0.10
0.20
0.30
0.40
0.50
0.60
0.70 In m⁻¹
ATTENUATION COEFFICIENT

fig. 21

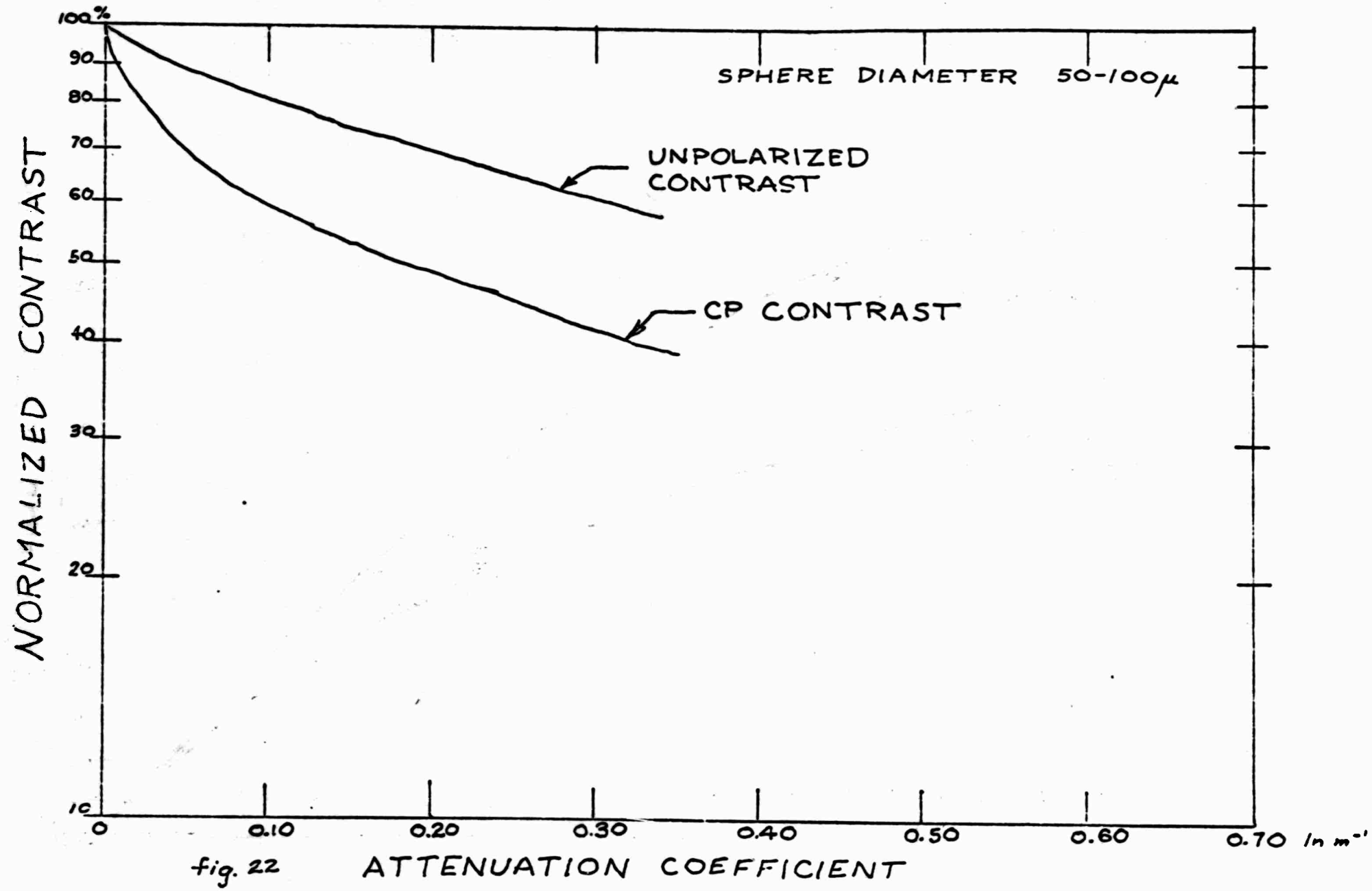
100%
90
80
70
60
50
40
30
20
10
NORMALIZED CONTRAST
SPHERE DIAMETER 50-100μ
UNPOLARIZED CONTRAST
CP CONTRAST
0
0.10
0.20
0.30
0.40
0.50
0.60
0.70 In m⁻¹
ATTENUATION COEFFICIENT

fig. 22

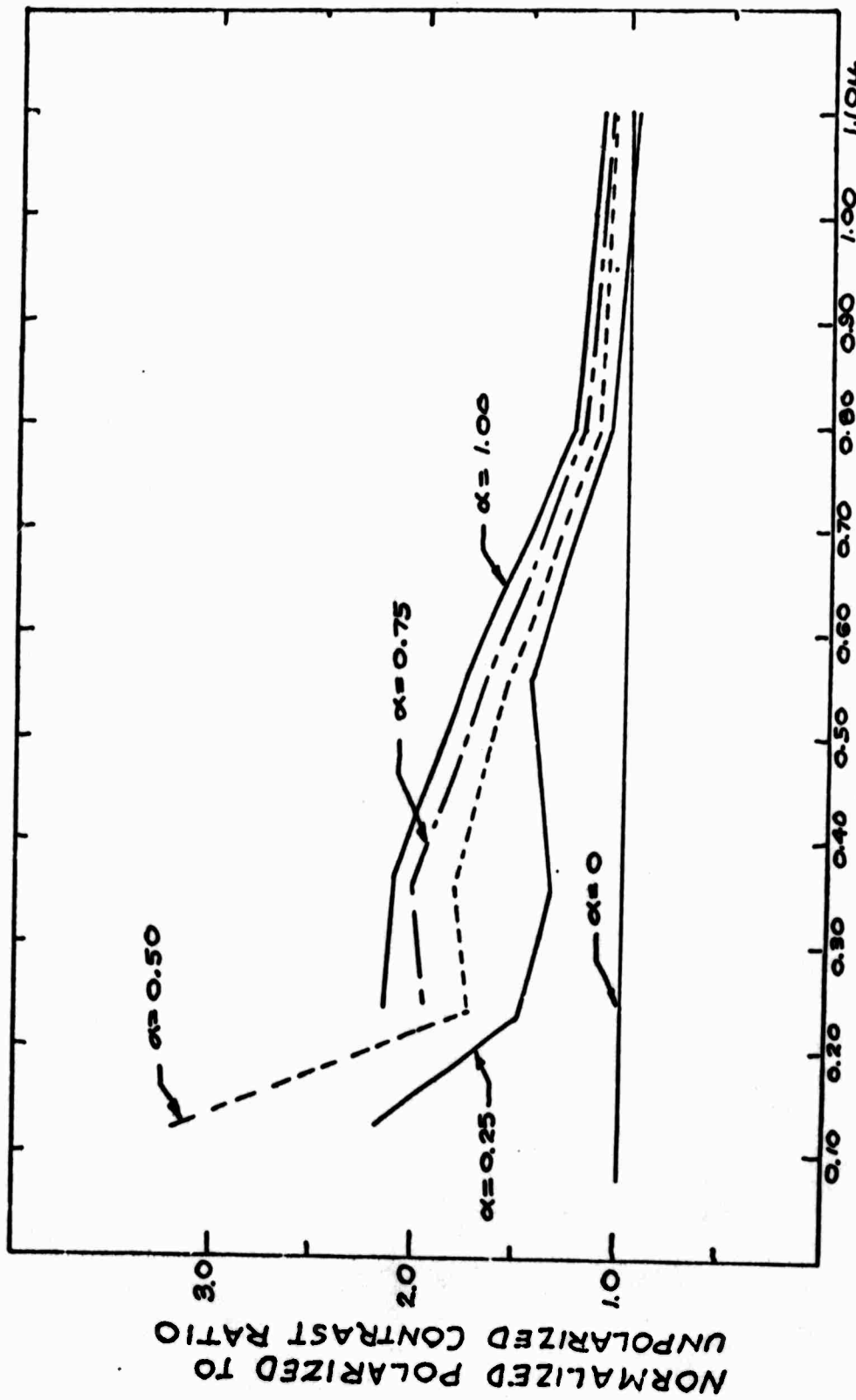
NORMALIZED POLARIZED TO
UNPOLARIZED CONTRAST RATIO
3.0
2.0
1.0
α=0.50
α=0.25
α=0
α=0.75
α=1.00
0.10
0.20
0.30
0.40
0.50
0.60
0.70
0.80
0.90
1.00
1.10μ
SCATTERING SPHERE DIAMETER

fig. 23

DISCUSSION

Chapter Five

The purpose of this work has been to investigate the conditionality of CP contrast improvement as a function of diameter and concentration. This study plus knowledge of natural scattering conditions conditions allows some qualitative remarks to be made concerning the effect of CP contrast improvement in the ocean.

To summarize the experimental results, it was found that for the nonaborbing polystyrene latex spheres with relative refractive index of M = 1.20, the apparent contrast of the white target to the background composed of the velvet backing and the scattered space light in the receiver's field of view, improved for all concentrations of scatterers with diameters of $d \leq 0.796\mu$. For the spheres of diameter $d = 1.099\mu$ the contrast was slightly improved for concentrations corresponding to the range of attenuations found in the ocean. For the scatterer distributions from 6-100μ diameter CP degraded contrast for all concentrations.

1. Extrapolation to Natural Ocean

To consider the applicability of CP contrast improvement to the varied waters of the ocean, it is necessary to first note:

(a) Those ocean areas where the concentration and

size of scatterers is of the same order as those experimental scatterers for which contrast was improved, and

(b) to more closely note what contrast is in relation to an optical system and to consider the trade offs necessary to use CP for contrast improvement.

The ocean may be roughly divided into two geological zones. These are coastal waters and open ocean. The open ocean may be further divided into three vertical zones, the surface water or euphotic zone, the middle water, and the bottom. Comparison of the scatterers found in each zone with the scatterers used in the experiment allow the following comments:

(a) Rivers and ocastal waters, i.e., usually within 10 to 20 miles of land near the mouths of rivers. These waters contain large amounts of terrogenious particulate matter ranging from clay, silt, and fine sand to plant and animal debris. The largest volume of particulate matter is contained in particles large compared to the wavelength of light (13, 14). The relative refractive index as given by Burt for the bulk of such material is about $m = 1.20$ (1). It is, therefore, highly unlikely that circular polarization will improve contrasts in such areas and will quite probably cause degradation.

(b) The surface waters or euphotic zone of the open ocean normally ranges from a few meters to about 100 meters below the surface. This layer is the most active

region of organic growth in the ocean because of the large availabe amounts of sun light. The most active organic growth activity is found in regions of diverging upwelling currents and plentiful nutrients. Conversely areas of converging downwelling currents represent very poor organic activity. The major scatterers are organisms with refractive indices in the range $1.0 \leq m \leq 1.15$. The majority are phyto plankton and range in size from bacteria $0.02\mu < d < 50\mu$, to diatoms and dinoglagellates of diameters $1\mu < d < 100\mu$. Volume attenuation measurements made in highly productive Aleutian waters for $\lambda = 489.3$ mμ show maximum values of 0.52 ln/meter, well within the range of attenuation covered in the experiment. It is very likely that there will be some contrast improvement in these waters especially for backscatter from the particles less than 1μ diameter.

(c) The middle waters of the ocean extend from 100 meters below the surface, the lower euphotic zone, to a few meters from the bottom. Since the average depth of the ocean is about 3800 meters, this region is roughly 97% of the ocean waters (21). The major light scatterers consist of detrital material settling from the surface waters. These have basically the same refractive index range $1.0 < m < 1.15$ as the surface particulate matter. Jerlov notes that the sinking rate of the smaller particles is much slower (on the order of weeks or months) than the larger particles (13). Because of this the particles found in this region are

predominately of diameters $d \leq 1\mu$. The volume attenuation coefficient for this region is generally very low, $0.05<\alpha<.10$ ln/meter, indicating that most state of the art underwater optical systems would be absorption-and not contrast-limited. For possible future higher-power systems circular polarization would definitely improve target contrast in this region of the ocean.

(d) Bottom waters range from several meters above the bottom to the bottom. Jerlov has sampled single layers of fine particles near the bottom of diameter (13). Observers from the Naval Electronic Laboratory, San Diego, have noted similar bottom layers of particulate matter while in the bathyscape Trieste. No estimates are known of the size of scatterers in these layers. However, Jerlov states that in geological bottom samples fine clay particles of diameter $1.0\mu \leq d \leq 3.0\mu$ and diatomaceous particles of diameter $d \sim 7.0 - 10.0\mu$ have been found. Although the particle size distributions are not known, some contrast improvement with circularly polarized light may be expected.

2. Application

Apparent contrast has been considered simply from a photometric measurement point of view. Apparent contrast ratios have been defined photometrically for varying sphere sizes and concentrations. However, for practical application of CP contrast improvement in any scattering medium, the real receiver's signal transfer characteristics must be

taken into account to predict visibility range.

The CP contrast improvement technique necessarily reduces the effective input signal power by 0.3 to as much as 1.2 log units depending upon the particular polarizers and filter disposition used. Because of this power reduction, the useful dynamic range of the receiver system must be considered.

Contrast improvement may be applied to two areas of interest for real receivers. The first is the area of improvement of image "visibility." The second is the increasing of visibility range. The following is meant only as a qualitative discussion of limitations to be expected when using the CP contrast improvement technique and is not meant to be an exhaustive treatise in either photographic or vidicon camera systems.

Real Receivers and Image Visibility. Let H represent input signal power (luminance, illuminance, etc.) and E output power then significant features of receivers are:

1. The saturation signal, H_s. The output signal does not change with additional amounts of input signal above H_s.

2. The threshold signal H_{th}. Input signals of lesser magnitude than H_{th} cause output signals to be buried in system noise and be undetectable.

3. The γ-characteristic slope of the receiver transfer curve defined as the ratio of change of the log of the output signal, E, to the log of the input signal, H.

4. The dynamic range of the receiver here defined as $\log H_s - \log H_{th} = \log H_s/H_{th}$. Signals in this range are recognized.

5. The receiver has a contrast sensitivity threshold increment ϵ. That is, the receiver cannot "resolve" targets with apparent contrasts less than ϵ.

For image visibility enhancement assume that the optical imaging system is located in water where circular polarization will increase apparent contrast by decreasing background. The receiver is working in its linear signal region. Without CP the image falling on the photo-active surface of the receiver has a white target to background illuminance ratio of $\frac{H_t}{H_b}$. The corresponding output signal ratio for the general receiver is $\frac{E_t}{E_b} = \left(\frac{H_t}{H_b}\right)^{\gamma}$. (For the vidicon television camera $\gamma = .65 - .70$, and for the photographic film γ is an experimental function of time $\gamma = \gamma_\infty (1 - e^{-kt})$ where γ_∞, k are characteristics of the particular film.)(6, 19).

Now when the CP contrast improvement technique is used, a CP filter is first placed on the source (assume perfect filters, 0.3 log units optical density). This reduces the output of an unpolarized source to 50% of its unpolarized luminous power. The logarithmic input signal to the receiver decreases by 0.3 log units. A CP filter analyzer is then put on the receiver. This reduces the luminous power from any Lambertian targets located in the receiver's field of view by at least 50% or 0.3 log units. Hence, the addi-

tion of the two CP filters to the system has caused the white target image illuminance, H_t, to be decreased by 0.6 log units from H_t. The background illuminance, H_b', has decreased by more than 0.6 log units because contrast has been improved. Hence, the new CP white target to background illuminance ratio in the image is greater than the old ratio $(H_t'/H_b') \geq (H_t/H_b)$ and three cases must be considered with regard to the signal transfer characteristic curve:

(a) If $H_b' > H_{th}$ and $(H_t'/H_b') > (H_t/H_b)$

(b) If $H_b' < H_{th}$ but $(H_t'/H_{th}) > (H_t/H_b)$

there will be a "visibility" improvement. However, if

(c) $H_b' < H_{th}$, but $(H_t'/H_{th}) < (H_t/H_b)$,

there will be a degradation in visibility because the receiver has now become power limited.

Photographic film typically has a linear input region (γ = constant) of about 1.3 to 1.5 log units (19). Output optical density ranges from 1.0 to 3.0 units depending upon the particular development time and type of emulsion. It may be easily seen that if the addition of the CP filters reduces the input signal by 0.6 log units and the white target to background illuminance ratio in the image is of the order of 1.0 to 2.0 log units, then the usefulness of

CP contrast improvement will be severely limited by the useful dynamic range of the film. This limitation on some types of film has been qualitatively observed in a few of the preliminary tests.

An artificially illuminated target against a watery background was viewed with CP and without, and a large improvement of contrast was noted. The same target was then photographed. The exposure of the film was below the film's threshold requirement and no target was observed. However, with a correct choice of film and a variable luminous output light source, the exposure of circularly polarized images can always be kept within the useful region of the film, giving improved visibility in the final photographs.

The vidicon camera has a useful dynamic input range of from 3.6 to 4.0 log units, and hence may be more likely to improve visibility under contrast limited conditions. The vidicon system accomplishes this wide dynamic range by having an electronic automatic photoconductive target voltage control (ATC) that compensates for light level changes caused by placing the CP filter in the system. However, because of the electronic nature of the system as the input sensitivity of the vidicon is increased, electronic noise increases also and a point is reached where any decrease in background seen on a TV monitor is matched by an increase in electronic noise-caused luminance.

To summarize, CP contrast improvement will enhance

if the addition of the CP filter doesn't lower
ound signal below the threshold or cause internal
oise to supplant background light as the contrast

isibility Range Considerations. Assume that the
receiver with the above mentioned characteristics
a small target illuminated by a light source lo-
to the receiver. The target has a diffuse Lam-
rface of reflectivity and is shown against a water
extending to infinity. The volume attenuation
t of the water is α. The target is located such
on the projection axis of the source and at a
in the source for field region. The light source
al luminous intensity of J_0. On the axis at a
from the source the luminous intensity is $J(r) =$
The target illuminance at the receiver collection
then $H_t = \frac{\rho A_t}{\pi} \frac{J_0 e^{-2\alpha r}}{r^4}$, a function of r.
nsider the transfer characteristic of the re-
e light source is circularly polarized with a
t the resulting input target signal be equal to
e receiver has no circular analyzer in place so
ively the input signal light is unpolarized. Let
arget signal be well above the input threshold,
sume that the receiver is contrast limited, so
$\frac{H_t - H_B}{H_B} = \epsilon$, the receiver's contrast sensitivity

threshold increment. If the target is moved any further from the receiver, H_t will decrease and the target will disappear.

The CP analyzer is put in place in the receiver and contrast is improved. The target may now be moved further away from the receiver until it either becomes contrast limited or the input target signal decreases below the threshold illuminance H_{th}.

The increase in range due to the contrast improvement is calculated as follows: Assume the receiver is contrast limited at the range r_o. The contrast of target to background is $\frac{H_t - H_B}{H_B} = \epsilon$, so that the background signal is $H_B = \frac{H_t}{\epsilon + 1}$.

A circular polarizing filter and analyzer is then placed over the receiver's collecting optics. This filter has a transmissivity for input unpolarized light of K where $0.0 < K \leq 0.5$. The filter improves the apparent contrast of the target by a contrast improvement ratio of R where $R\epsilon$ is the CP contrast. Letting primes ' denote CP illuminance the input target signal is now $H_t'(r_o) = K\, H_t(r_o)$. The new background illuminance is $H_B'(r_o) = \frac{H_t'(r_o)}{R\epsilon + 1}$ and is unchanged with range r. The target range may now be increased until the target illuminance decreases to cause the system to again become contrast limited at distance r_1. Then $H_t'(r_1) = (\epsilon + 1)\, H_B'(r_o)$, or $H_t'(r_1) = \frac{\epsilon + 1}{R\epsilon + 1} H_t'(r_o)$.

Putting into logarithmic form and simplifying we get an equation for r_1, the new contrast limited range, in terms of the old contrast limited range r_o and the contrast improvement ratio R

$$4 \ln r_1 + 2\alpha r_1 = 2\alpha r_o + 4 \ln r_o + \ln \frac{R\epsilon + 1}{\epsilon + 1}$$

This equation must be solved graphically. This was done for some of the experimental data.

Calculations were made of the anticipated visibility range improvement caused by CP contrast improvement for the 0.126μ, 0.234μ, 0.557μ, and the 0.796μ diameter sphere experimental data. For this calculation the contrasts for all sphere were taken for concentrations near α= 0.50 ln unit/meter; and the measured unpolarized contrast was substituted for ϵ. This means that the distance calculated will be that distance at which the CP contrast equals the unpolarized contrast at the old distance r_o= 0.603 meter.

The results of the calculations are presented in the table below.

T A B L E I V

Sphere Diameter	α (ln/m)	r_o(m)	CP Contrast	Unpolarized Contrast	r_1(m)	$100\frac{r_1}{r_o}$
0.126	0.508	.603	69.0	11.6	0.845	41.5%
0.243	0.606	.603	73.1	30.0	0.73	21.0%
0.557	0.479	.603	64.0	41.7	0.665	10.0%
0.796	0.519	.603	48.8	32.6	0.655	8.7%

In the table r_1 is the new distance.

As may be seen from the table the usefulness of CP for increasing visibility range decreases as increasing sphere size.

3. Summary

A contast improvement method has been conceived for underwater lighting and viewing systems using circular polarizing filters. In preliminary work it was discovered that CP for improving contrast appeared to be conditionally dependent upon scattering properties of the water in which the system was used.

Circular polarization would improve contrast under one set of receiver-water conditions and have no noticeable effect in another set. An investigation was conducted in two parts: (1) to determine significant light scattering properties of natural waters by a literature search. Specifically, these properties were the size, concentration (or light attenuation) and refractive index ranges of the natural scatterers. (2) to conduct an engineering study in which the degradation of apparent contrast of a Lambertian target could be noted in waters with known scattering properties similar to those encountered in natural waters.

In the literature search it was found that for 97% of the ocean's volume, small particles of diameter near 1μ, with relative refractive indices between 1.00 and 1.15, predominate in number and quite possibly in total scattering

effect.

In the experimental work spherical scatterers of sizes ranging from 0.1μ to 100μ with a relative refractive index of 1.20 were used for contrast degradation. It was found that circular polarization of source and receiver definitely improved contrasts of a white Lambertian target for all spheres with diameters less than 0.796μ for all concentrations. Scattering spheres of diameter 1.0μ showed a very slight contrast improvement for attenuation coefficients between 0.25 — 1.0 ln/meter. For spheres of diameters from 6-100μ diameter, circular polarization caused a degradation in contrast.

Comparing the information obtained on the ocean's natural scattering particle distribution with the experimental study, it was determined that circular polarization could improve the apparent contrast of an image falling on the photo-sensitive area of an optical receiver. However, it was then noted that the "visibility" enhancement of image or an increase in visibility range could only be accomplished if the signal transfer characteristics of receiver were considered. If the addition of the circular polarizing filters to a system caused the system to become power limited then no benefit would be derived from the addition of the filters. For a vidicon television camera tube, a decrease in input signal light flux when adding the CP filters could cause the TV system electronic noise to supplant the backscattered

light flux as the contrast limiter.

A simple mathematical model of the target and background-caused receiver illumination was constructed to show possible improvements in visibility range for some of the experimental data. For the model and the data chosen, range improvement was from 9 to 40%.

It is important that the effect of circular polarization for contrast improvement be found for the 97% of the ocean where the small scatterers abound, as it is quite possible that future Deep Submergence Vehicles will operate in this region with blue-green laser light sources. Both optical imaging systems and optical radar systems are feasible. Since lasers are necessarily sources of linearly polarized light, the conversion of this light to circularly polarized light could be accomplished by the addition of a $\frac{1}{4}$-wave retarder with negligible power loss. The only lossy element in a CP laser-receiver system would be a CP filter on the receiver, resulting in a signal power loss of only 0.3 to 0.5 log units.

BIBLIOGRAPHY

1. Burt, Wayne Vincent. Scattering of Light in Turbid Water. Ph. d. in Oceanography. University of California, Los Angeles, May 1965.

2. Born, Max and E. Wolf. Principles of Optics. 3rd Ed., N. Y., Pergamon Press, 1965.

3. Dietrich, Gunter. General Oceanography. N. Y., Wiley, 1963.

4. Duntley, S. Q. "Light in the Sea." J. Opt. Soc. Am. v.53, n.2, pp 214-233, Feb. 1963.

5. Duntley, S. Q., A. Boileau, and R. Priesendorfer. "Image Transmission by the Troposphere I." J. Opt. Soc. Am. v.47, n.6, pp 499-506, June 1957.

6. Fink, Donald G. editor. Television Engineering Handbook. N. Y., McGraw-Hill, 1957.

7. Gilbert, G. D. and J. C. Pernika. "Improvement of Underwater Visibility by Reduction of Backscatter with a Circular Polarization Technique." Applied Optics. v.6, p. 741, April 1967.

8. Gilbert, G. D. "Deep Sea Light Attenuation Measurements at 2000 Meter Depths." U. S. Naval Ordnance Test Station, China Lake, Calif., Technical Report, (NOTS TP 3994) Dec. 1965

9. Gilbert, G. D. and R. O. Rue, "Light Attenuation Measurements off the coast of Baja California." U. S. Naval Ordnance Test Station, China Lake, Calif., Technical Report, (NOTS TP 4343) May 1967.

10. Gray, Dwight E. Coord Editor. American Institute of Physics Handbook. 2nd Ed., N. Y., McGraw-Hill, 1967, pp. 6-77, 79.

11. Hughes, R. S. and R. W. Austin. "Deep Sea Light Attenuation Measurements with a Null Balance Transmissometer." U. S. Naval Ordnance Test Station, China Lake, Calif., Technical Report, (NOTS TP 3748) Feb. 1965.

12. Hulbert, E. O. "Optics of Distilled and Natural Water." J. Opt. Soc. Am. v.35, pp. 698-705, Nov. 1945

13. Jerlov, Nils G. "Optical Studies of Ocean Waters." Reports of the Swedish Deep-Sea Expedition. v.3, 1951.

14. Jerlov, Nils G. "The Particulate Matter in the Sea as Determined by means of the Tyndall Meter." Tellus. v.7, p.218, 1955.

15. Kingslake, Rudolf. editor. Applied Optics and Optical Engineering. N.Y., Academic Press, v.1, pp. 6-7, 1965.

16. Mauro, Joseph. General Electric Optical Engineering Handbook. Syracuse, N.Y., G.E. Corp., 1962.

17. Morrison, Robert E. Studies on Optical Properties of Sea Water at Argus Island in N. Atlantic Ocean and in Long Island and Block Island Sounds. Ph.D. in Oceanography. New York University, June 1967.

18. O'Neill, Edward L. Statistical Optics. Palo Alto, Calif., Addison-Wesley, 1963.

19. Shaftan, Kenneth and D. Kawley. Photographic Instrumentation. Redondo Beach, Calif., Soc. Photo. Inst. Engrs., 1962,p.110.

20. Shurcliff, William A. Polarized Light. Cambridge, Mass., Harvard University Press, 1962.

21. Sverdrup, H. V., M. W. Johnson, R. V. Fleming. The Oceans. N. J., Prentice-Hall, 1942.

22. Tolbert, W. H. "On the Concentration and Size Distribution of Particulate Matter in Sea Water." U. S. Naval Mine Defense Lab. Panama City, Fla., Tech. Paper, (TP 168) Aug. 1959.

23. Tyler, J. E. "Monochromatic Measurement of the Volume Scattering of Natural Waters." J. Opt. Soc. Am. v.47, pp. 745-747, Aug. 1957.

24. Tyler, J. E. "Scattering Properties of Distilled and Natural Waters." Limnology and Oceanography. v.6., pp. 451-456, Oct. 1961.

25. Tyler, J. E. and R. W. Priesendorfer. "Light in the Sea." The Sea. M. N. Hill, editor, N. Y., Wiley, 1962.

26. Van De Hulst, H. C. Light Scattering by Small Particles N.Y., Wiley, 1967.

27. Weast, Robert C. ed. in chief. Handbook of Chemistry and Physics. 48th Ed., Cleveland, Ohio, Chemical Corp., 1967.

UNCLASSIFIED
Security Classification

DOCUMENT CONTROL DATA - R & D

(Security classification of title, body of abstract and indexing annotation must be entered when the overall report is classified)

1. ORIGINATING ACTIVITY *(Corporate author)*

Naval Weapons Center
China Lake, California 93555

2a. REPORT SECURITY CLASSIFICATION

UNCLASSIFIED

2b. GROUP

3. REPORT TITLE

INVESTIGATION OF CONTRAST DEGENERACY WITH INCREASING SCATTER CONCENTRATION FOR A WATER MEDIUM WHEN ILLUMINATED WITH AND WITHOUT A CIRCULARLY POLARIZED SOURCE

4. DESCRIPTIVE NOTES *(Type of report and inclusive dates)*

Facsimile of thesis

5. AUTHOR(S) *(First name, middle initial, last name)*

Gary D. Gilbert

6. REPORT DATE	7a. TOTAL NO. OF PAGES	7b. NO. OF REFS
December 1968	74	--

8a. CONTRACT OR GRANT NO.	9a. ORIGINATOR'S REPORT NUMBER(S)
b. PROJECT NO.	NWC TP 4681
c.	9b. OTHER REPORT NO(S) *(Any other numbers that may be assigned this report)*
d.	--

10. DISTRIBUTION STATEMENT

THIS DOCUMENT IS SUBJECT TO SPECIAL EXPORT CONTROLS AND EACH TRANSMITTAL TO FOREIGN GOVERNMENTS OR FOREIGN NATIONALS MAY BE MADE ONLY WITH PRIOR APPROVAL OF THE NAVAL WEAPONS CENTER.

11. SUPPLEMENTARY NOTES	12. SPONSORING MILITARY ACTIVITY
	Naval Material Command Naval Ordnance Systems Command Washington, D.C. 20360

13. ABSTRACT

ABSTRACT. Luminous flux returns were measured from a black and white painted 5-inch x ½-inch aluminum target placed in a water filled 60 x 30 x 25 cm aquarium illuminated by an external circularly polarized (CP) tungsten projector lamp. Simultaneously, apparent background flux containing backscatter from the illuminating beam was measured with and without a circular analyzer on the Model 2000 Gamma-Scientific telephotometer. Turbidity of the water was controlled by adding varied sizes of polystyrene latex spheres of relative refractive index m = 1.20. Contrasts were determined as a function of particle diameter and amount concentration for six discrete-size spheres ranging from 0.126 microns to 1.099 microns and three size distributions from 6 to 100 microns.

A ratio comparison of the contrasts showed a definite improvement for the smaller diameter spheres, d = 0.557 microns with circularly polarized light. There was only a slight contrast improvement for the 0.796 micron spheres and no improvement for the 1.099 micron spheres. Contrast degraded for CP illuminated scattering from spheres in the 6 to 100 micron diameter range. Considering the ocean's natural scatterers distribution, circular polarization will probably most improve contrast in the vertical region from the lower euphotic zone to a few meters above bottom.

This report is a facsimile of a thesis prepared in partial satisfaction of the requirements for a master's degree of science in engineering. It is published at the working level for information only.

DD FORM 1 NOV 68 1473 (PAGE 1)

S/N 0101-807-6801

UNCLASSIFIED
Security Classification

14 KEY WORDS	LINK A		LINK B		LINK C	
	ROLE	WT	ROLE	WT	ROLE	WT
Underwater visibility Luminous flux returns Circularly polarized light Contrast improvement						